Valley-bottom wetland agricultural conversion and recovery shape greenhouse gas dynamics and soil carbon sequestration in an African tropical highland system

Sharon Gubamwoyo[1,9], Sonja M. Leitner[2], Gabriele Weigelhofer[1,3], Damaris G. Kisha[4,5], Oswald Omuron[6], Dominik Henrik Zak[7], Thomas Hein[1,8], Gretchen M. Gettel[4,6]

[1]Institute of Hydrobiology and Aquatic Ecosystem Management, Department of Ecosystem Management, Climate and Biodiversity, BOKU University, Gregor-Mendel-Straße 33, 1180 Vienna, Austria
[2]Mazingira Centre for Environmental Research and Education, International Livestock Research Institute (ILRI), Naivasha Rd, PO 30709, 00100 Nairobi, Kenya
[3]Wasser Cluster Lunz, 3293 Lunz am See, Austria
[4]IHE-Delft Institute for Water Education, Westvest 7, 2611 AX Delft the Netherlands
[5]International Crane Foundation, P.O. Box 76668-00508, Nairobi, Kenya
[6]Department of Ecoscience, Freshwater Ecology, Aarhus University, C. F. Møllers Allé 3, 8000 Aarhus, Denmark
[7]Department of Ecoscience, Catchment Analysis and Environmental Management, Aarhus University, C. F. Møllers Allé 3, 8000 Aarhus, Denmark
[8]Christian Doppler Laboratory for Meta Ecosystem Dynamics in Riverine Landscapes, BOKU University, Institute of Hydrobiology and Aquatic Ecosystem Management, Department of Ecosystem Management, Climate and Biodiversity, Gregor-Mendel-Straße 33, 1180 Vienna, Austria
[9]National Water and Sewerage Corporation (NWSC), Water Quality Department, P.O BOX 7053, Kampala, Uganda

Correspondence to: Sharon Gubamwoyo (s.gubamwoyo@students.boku.ac.at; sharonguba@gmail.com)

Abstract. Tropical wetlands significantly impact global greenhouse gas (GHG) budgets and carbon storage: however, data from sub-Saharan African (SSA) remain limited. Highland valley-bottom wetland (HVBW) agriculture supports millions, yet its effects on GHG emissions and carbon storage remain undocumented. This study quantified soil emissions of nitrous oxide (N_2O), carbon dioxide (CO_2), and methane (CH_4) in the Taita Hills, Kenya, from 12 converted, 10 recovering, and one reference (intact) HVBWs. Agricultural conversion shifted wetland emissions from CH_4 to N_2O dominance. Converted HVBWs were N_2O sources (2.7 kg N_2O-N $ha^{-1}yr^{-1}$), driven by elevated soil nitrate, whereas the intact wetland was an N_2O sink (−0.3 kg N_2O-N ha^{-1} yr^{-1}), with high soil moisture and high soil C/NO_3^--N ratio suggesting complete denitrification. Recovering HVBWs showed intermediate N_2O emissions (0.6 kg N_2O-N ha^{-1} yr^{-1}). CO_2 emissions were similar between converted and recovering HVBWs (10,850 vs. 11,031 kg CO_2-C ha^{-1} yr^{-1}) but lower in the intact (2,923 kg CO_2-C ha^{-1} yr^{-1}). CH_4 emissions were highest in the intact HVBW (2,757 kg CH_4-C ha^{-1} yr^{-1}), intermediate in recovering sites (879 kg CH_4-C ha^{-1} yr^{-1}), and lowest in converted sites (37 kg CH_4-C ha^{-1} yr^{-1}). The intact HVBW had 224 Mg C ha^{-1}, indicating carbon loss rates of 2.6 Mg C ha^{-1} yr^{-1} over 45 years for converted HVBWs. Restoring Taita Hills wetlands would sequester 1.1 Mg C ha^{-1} yr^{-1}, offsetting ~0.0005% of Kenya's annual agricultural GHG emissions, or 9.8% when scaled nationally. These findings highlight

trade-offs between GHG emissions and carbon storage in HVBWs, with wetland recovery promoting functional restoration and long-term carbon sequestration in SSA.

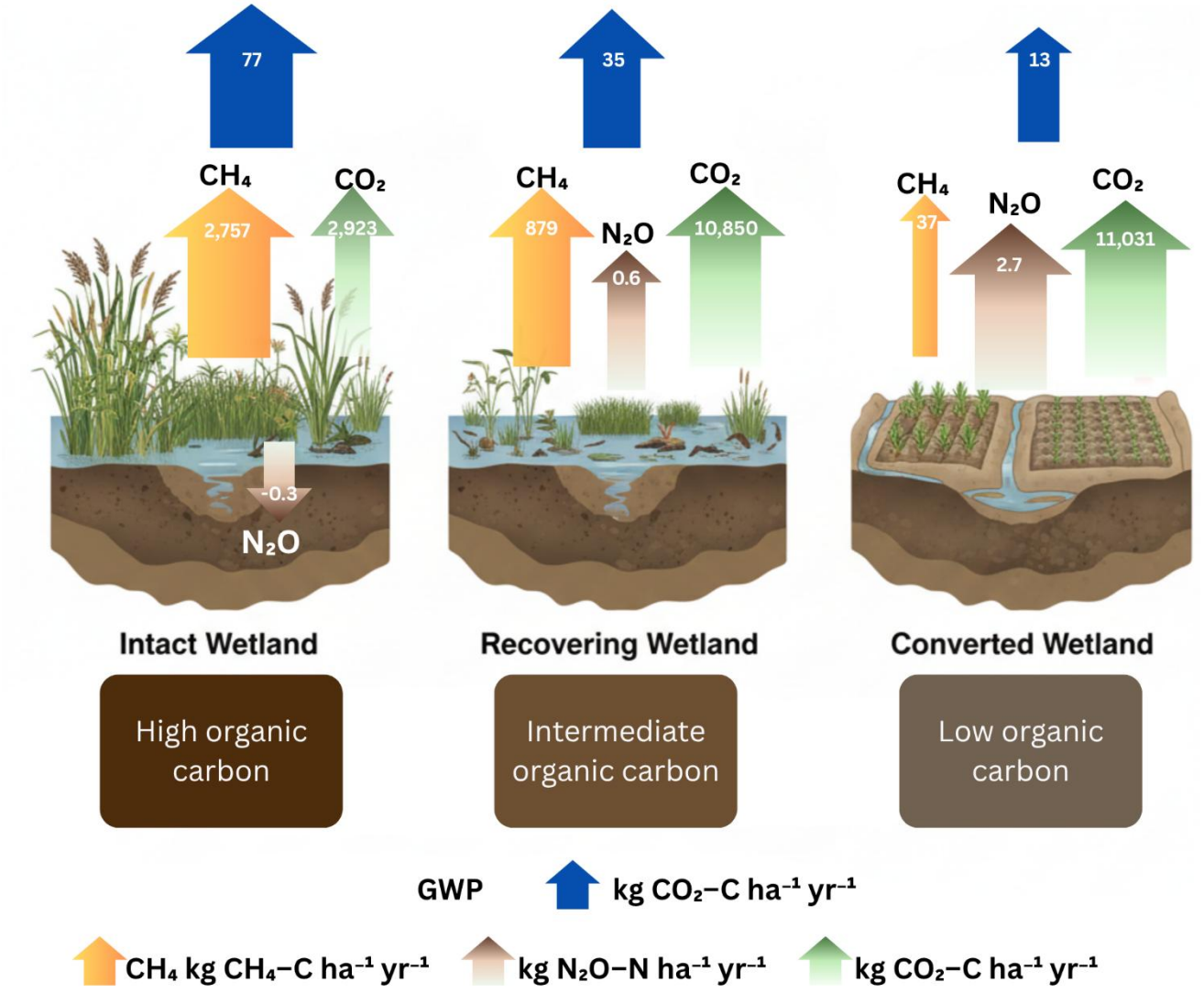

1 Introduction

Globally, agriculture is estimated to cover 40% of the Earth's land and is a major driver of wetland loss, leading to reduced soil organic carbon (SOC) stocks and increased greenhouse gas (GHG) emissions (Jia et al., 2022; Li et al., 2024, 2025). Wetlands cover approximately 5-7% of Sub-Saharan Africa (SSA), store approximately 155 Gt of SOC, and are vital to the livelihoods of millions of people (Dube et al., 2023; Jones et al., 2016). African wetlands play a crucial role in providing ecosystem services, including agricultural production, water provisioning, flood protection, biodiversity, and climate regulation (Convention on Wetlands, 2025; Rebelo et al., 2010; van Dam et al., 2013). In recent decades, Africa has experienced a 50% loss of wetlands, surpassing the global loss rate of 35%, primarily driven by conversion to agriculture (Dube et al., 2023; Fluet-Chouinard et al., 2023; Ramsar Convention on Wetlands, 2018). Wetlands can be exceptionally fertile, with with soils that remain saturated and nutrient-rich throughout the year (Beuel et al., 2016), and are often converted to agriculture when upland soils under low-intensity cultivation no longer support yields needed to sustain growing populations (Garba et al., 2025).

Highland Valley-Bottom Wetlands (HVBWs), located in montane systems above ~1200 m.a.s.l., are an important component of the highland perennial farming system, which cover 39.3 million ha and supports 82.5 million people in Sub-Saharan Africa (Lynam, 2020). African montane systems are ecologically distinct and valued for their water resources and biodiversity (Njana, 2025; Simango, 2024). In East Africa, HVBWs support more than 65% of local communities through agriculture, either financially or directly through the provision of food (Lynam, 2020; Marinus, 2021), and are increasingly under pressure due to population and economic growth as well as drying lowlands caused by climate change (Gubamwoyo et al., 2025). Specifically, this leads to changes in hydrological flow-paths for flood management and irrigation, increased nutrient loading via manure or synthetic fertilizer application, and the alteration of wetland geomorphology (Gubamwoyo et al., 2025; Li et al., 2025). These changes alter GHG emissions and SOC stocks and are commonly associated with reduced CH_4 emissions but increased CO_2 and N_2O emissions, with residual CH_4 emissions often restricted to drainage ditches (Gardner & Finlayson, 2018; Peacock et al., 2021; Tangen & Bansal, 2020). As a result, the relative contributions of CH_4, CO_2, and N_2O to annual GHG emissions shift substantially (Anthony & Silver, 2021; Li et al., 2024; Nahlik & Mitsch, 2011; Xu et al., 2019). Despite the importance for livelihoods and to climate feedbacks, the impact of land use change on SOC stocks and GHG emissions in HVBWs has not been previously studied. GHG dynamics in wetland soils are controlled by biogeochemical processes that regulate CO_2, CH_4, and N_2O production and consumption. These processes are influenced by proximate and distal factors (Malak et al., 2021), which are essential for developing effective mitigation strategies. Proximate controls directly impact GHG emissions and include biogeochemical and physicochemical properties such as organic matter, nutrients, dissolved oxygen, and temperature (Pasut et al., 2021; Turetsky et al., 2014; Yang et al., 2025). Distal controls indirectly affect GHG emissions by altering hydrology and nutrient concentrations through factors such as land-use change and hydrogeomorphology (Turetsky et al., 2014). Soil respiration generates CO_2, while CH_4 is produced through methanogenesis mainly under waterlogged, oxygen-depleted conditions and is oxidized when the soil becomes aerated (Mander et al., 2025). N_2O is produced

via nitrification and denitrification, with related pathways, such as nitrification-denitrification and Dissimilatory nitrate reduction to ammonium (DNRA), also contributing to its production (Bahram et al., 2022; Vymazal, 2025). Under carbon-rich, low-nitrate conditions, typical of intact wetlands, complete denitrification can reduce N_2O to N_2, thereby limiting N_2O accumulation. In HVBWs, these controls differentiate intact, recovering, and converted wetlands: conversion for agricultural land use increases aeration and nitrate availability, enhancing CO_2 and N_2O emissions while suppressing CH_4 production (Turetsky et al., 2014), whereas intact wetlands maintain saturated anaerobic soils, favouring CH_4 generation and limiting CO_2 and N_2O release (Murguia-Flores et al., 2023; Shah et al., 2024). Recovering wetlands (wetlands that were abandoned for a few months to years to decades) display intermediate conditions as soil processes gradually shift toward those of intact wetlands. SOC stocks are highest in intact wetlands and decrease in converted systems due to cultivation, soil disturbance, and degradation (Shi et al., 2024; Tangen & Bansal, 2020).

The Taita Hills of southern Kenya are a "water tower system" (Kenya Water Towers Agency, not dated) that supports the region's water supply. The HVBWs within this and other systems sustain over 95% of the livelihoods in Taita Taveta County through their organic-rich, fertile soils, water availability, and flat topography. In addition, the Taita Hills harbour several endemic plant and animal species owing to their unique ecology of long-term isolation and varied microclimates. Therefore, they are recognized as Key Biodiversity Areas and are included in international conservation initiatives like invasive species awareness and forest management (Mwacharo, 2024).

This environment promotes organic matter accumulation, thereby supporting high SOC levels and contributing to long-term carbon storage. According to Njeru et al. (2017), in the Taita Hills, higher elevations are associated with increased SOC levels, attributed to cooler temperatures and greater rainfall. The study further noted that land-use conversion led to a significant ~ 50% loss of SOC and a corresponding increase in CO_2 emissions. As agricultural pressure and climate change intensify in the region, understanding the GHG emissions and SOC dynamics of these wetlands is crucial for sustainable wetland management and evidence-based climate policy-making. Although studies have been conducted in forests within Taita Hills, detailed investigations of GHG dynamics and SOC storage in the HVBW remain limited.

We compared GHG emissions and SOC stocks in three types of HVBWs: those actively used for agriculture (converted HVBWs), those abandoned for years to decades (recovering HVBWs), and those never used for agriculture (intact HVBWs). This study focused on field-based GHG measurements, aiming to i) compare GHG fluxes and their potential biogeochemical controls seasonally and spatially between intact, recovering, and converted HVBWs in small headwater catchments in Taita Hills, Kenya, and ii) quantify cumulative GHG emissions and relate them to SOC stocks at the catchment level. We hypothesized that i) converted HVBW are major sources of N_2O and CO_2, especially during the growing seasons due to fertilizer N inputs, but act as sinks for CH_4 due to mostly aerobic soil conditions; ii) intact HVBWs are major sources of CH_4 and minor sources of CO_2 with no N_2O emissions under natural hydrological soil conditions that are mostly anaerobic; iii) recovering HVBW are expected to show CH_4 and N_2O fluxes shifting toward those of intact HVBWs as soils transition from oxic, drained conditions to more reduced, water-saturated states; and iv) SOC stocks are highest in the intact HVBWs and

lowest in the converted HVBWs due to continued cultivation, soil compaction, and increased soil organic matter decomposition.

2 Materials and Methods

2.1 Study area

This study was conducted in the Taita Hills (3°25´S,38°20´E) in Taita-Taveta County, southeastern Kenya, which form an integral part of the Eastern Arc Mountains, renowned for their rich biodiversity (Platts et al., 2011). The Taita Hills cover an area of approximately 1000 km^2 at an elevation ranging from ~1200 – 2200 m a.s.l. The geological structure of the Taita Hills comprises banded biotite gneiss and undifferentiated Precambrian formations. These are accompanied by fertile Cambisols and humic Histosols, which are derived from the weathering of gneiss, making the area suitable for agriculture (Horkel et al., 1979; Pellikka et al., 2009). Most of the study area is characterised by humic Cambisols and Umbrisols, particularly at higher elevations (Mganga et al., 2022; Njeru et al., 2017). The Hills experience two primary rainy seasons, with prolonged rainfall from March to June and shorter, more intense rainfall from October to December, with January and February are the driest months (Gubamwoyo et al., 2025; Pellikka et al., 2018). On average, the highlands receive more rainfall (1900 mm p.a) than the lowlands (440 mm p.a) (Taita Taveta County Government, 2023).

The study was conducted in the highland valley-bottom wetlands (HVBW) of Wundanyi and Mwatate (Wundanyi: ~ 117 km² and Mwatate: ~ 57 km²) sub-catchments (Figure 1, Table S1). These wetlands comprise patches of less than 5 ha and are heavily used by smallholder farmers (Gubamwoyo et al., 2025). The two sub-catchments are dominated by various agricultural practices carried out by small-scale farmers (Table S1; Gubamwoyo et al., 2025).

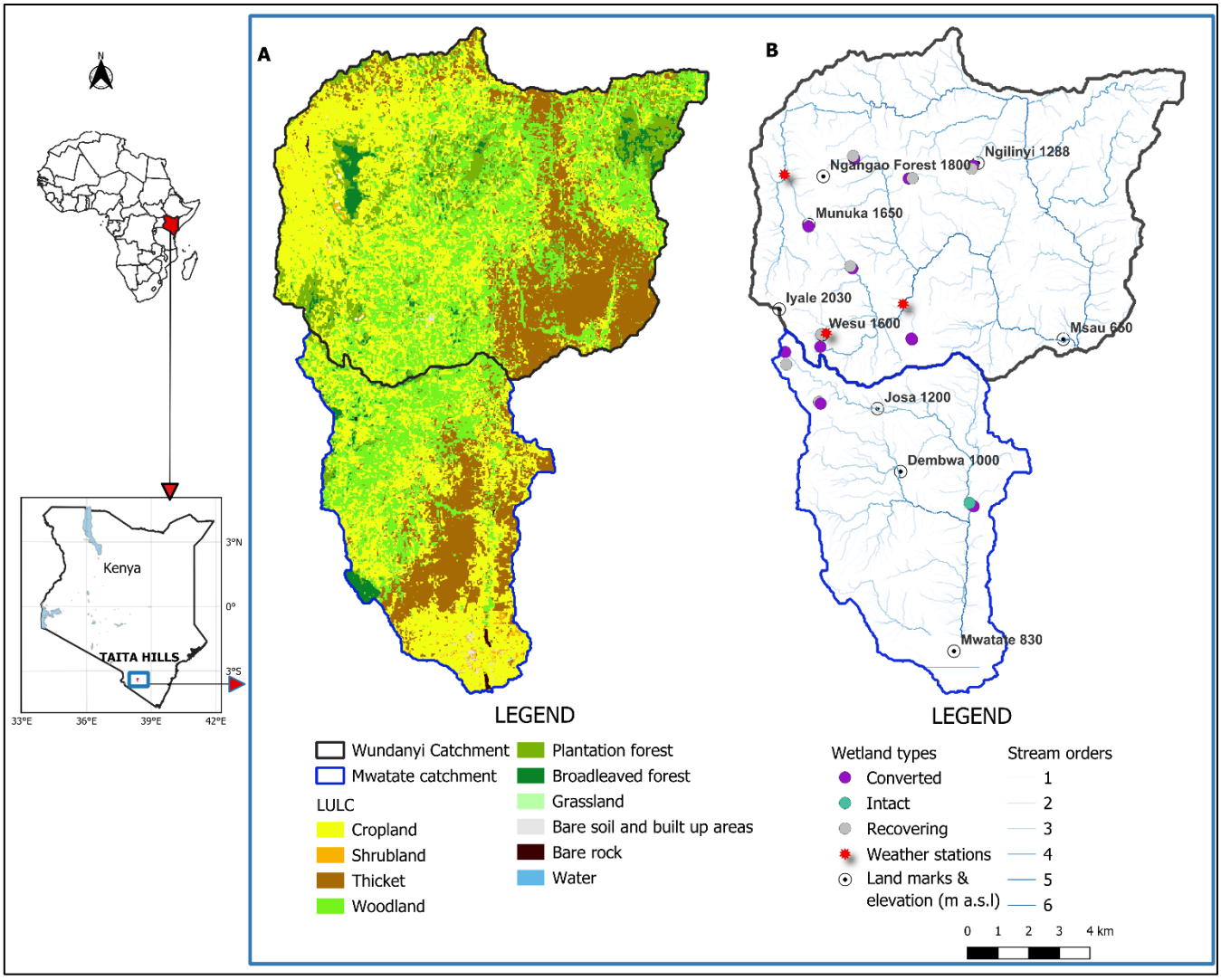

Figure 1: *Map of the Wundanyi and Mwatate sub-catchments. (A) Land use and land cover (LULC) in the two sub catchments and (B) the stream network, studied Highland Valley-Bottom Wetland, weather stations, and landmarks with their peak elevation in m a.s.l. The scale represents the extent of the Taita Hills sub-catchments and does not apply to the inset map of Africa or Kenya.*

2.2 Sampling design

To understand the temporal and spatial variation of GHG emissions in the HVBWs, bi-weekly measurements of GHG fluxes and soil parameters were carried out between November 2022 and January 2023 and April 2023 to April 2024 (16 months), resulting in a total of 28 sampling campaigns across 23 sites: 12 converted HVBWs, 10 recovering HVBWs, and one intact HVBW (Table S1). Wetland sites were classified as recovering, intact, and converted based on a combination of two

complementary lines of evidence. First, the LULC time series (1987–2023; Section 2.1.2) was used to trace each site's land-use history, distinguishing areas with a documented history of conversion to agriculture from those without. Second, semi-structured interviews with farmers and local authorities (Section 2.1.3; Gubamwoyo et al., 2025) provided information on prior disturbance, abandonment, and any restoration or management interventions at the site level. Converted HVBWs were defined as wetlands that are currently under agricultural use and range in age since conversion from 1963 to 2023 (Gubamwoyo et al. 2025; Table S1). Recovering HVBWs were defined as wetlands that were used for agriculture in the past but have been abandoned for ≥ 5 years due to high soil moisture or frequent flooding and have regained natural wetland vegetation (Gubamwoyo et al., 2025). The intact HVBW, which had never been used for agriculture, was studied. It was permanently flooded and predominantly covered by *Typha latifolia* vegetation, whereas the recovering HVBWs were partially flooded with some parts wetter than others, mainly dominated by *Cyperus odoratus,* except for two sites that were dominated by ferns (*Pteris catoptera*). The converted HVBWs generally comprised drier soils, with a few sections having soil moisture exceeding 30 %. Crops grown in the converted wetlands include maize, beans, kale, nightshade, French beans, peas, arrowroot, and spinach (Gubamwoyo et al., 2025). Each sampling site consisted of two random sampling patches, with three GHG chamber bases installed in each patch for GHG sampling (Section 2.4).

2.3 Meteorological data

Air temperature and rainfall data over time were collected from two local weather stations (Basic Weather Station / BWS200, USA) located at representative locations of the Taita Hills, monitored by the Taita Research Station under the University of Helsinki (Figure 1). Daily precipitation was measured using a tipping bucket gauge (Arg100), and the air temperature was measured using a temperature sensor (RH-Capac CS215).

The study covered 2.5 dry seasons from January to mid-March 2023 and 2024 and from June to September 2023. The dry seasons ended with the onset of the first rain of the subsequent wet seasons, starting in mid-March 2023 and lasting until May (long rains season) and mid-October to mid-December (short rains; Figure S4). Rewetting events within the study period were defined in two ways: first, as rain events occurring during the dry season after 10 consecutive days of no rain, and second, as the first rain event at the onset of the rainy season. There was a total of 20 days of rewetting days in the dataset, which were identified in April, July, August, September 2023, and March 2024.

2.4 Soil GHG sampling, analysis, and calculation

2.4.1 Soil GHG sampling

Soil-atmosphere fluxes of CH_4, CO_2, and N_2O were measured using the closed static chamber method with manual gas sampling combined with gas chromatography analysis (Butterbach-Bahl et al., 2016; Rochette, 2011) for the first 24 sampling campaigns, and using the closed static chamber method combined with portable LI-COR analyzers (LI-7820 N_2O/H_2O Trace Gas Analyzer for N_2O and LI-7810 $CH_4/CO_2/H_2O$ Trace Gas Analyzer for CH_4 and CO_2; LICORbio, Lincoln, USA) for the

last four sampling campaigns. Parallel measurements using both methods (gas vials/GC and LI-COR) were performed during the twentieth sampling campaign per gas to ensure comparability. Linear regression showed good agreement between methods for all three gases (CH_4 (R^2 = 0.81), CO_2 (R^2 = 0.97), and N_2O (R^2 = 0.84), indicating no systematic bias between the two measurement approaches. Before the measurements, three opaque open chamber bases made from PVC (area = 0.10 m², height = 0.15 m) were inserted to a depth of 5 cm into the soil at different site patches two weeks before the start of the sampling campaign (Figure S4; Parkin & Venterea, 2010). Chambers were installed on bare soil, and when necessary, vegetation was removed and the soil was allowed to equilibrate for a week following installation. Furthermore, during the sampling campaigns, vegetation was removed, when necessary, within the chamber base areas to ensure that we measured the soil fluxes. The mean chamber base height was measured during each sampling campaign to account for changes and minimize errors when calculating the total chamber headspace. The intact HVBW was permanently flooded (> 40 cm water depth); therefore, a 30 m wooden walkway was installed to avoid disturbing the sediment during sampling, and a floating chamber was used (Figure S2).

For gas sampling, chamber lids (area = 0.10 m², height = 0.12 m) were used to close the chamber bases and enable gas collection from the chamber headspace (Figure S3). The chamber lids were lined with a thin rubber seal to ensure airtight sealing and were held to the bases with fold-back binder clips to prevent leakage. In addition, the chamber lids were covered with reflective tape to reduce excessive heating from the incoming solar radiation. Each chamber was fitted with a pressure equilibration tube, an air circulation fan, a thermometer port to measure the headspace temperature during sampling, and a gas sampling point (Butterbach-Bahl et al., 2016; Hutchinson & Livingston, 2001; Zheng et al., 2008; Figure S2). For the floating chamber, Styrofoam was lined with silver tape, and the chamber lid was fitted on top of it, leaving the hollow space open. The gas outlet sampling point was fitted with a transparent PVC pipe (0.5 mm diameter, 1 m length) to enable sampling, where the samples were collected after flashing the tube once.

For manual gas sampling (the first 24 sampling campaigns), gas pooling from three replicate chambers was performed (Butterbach-Bahl et al. 2016). This involved collecting 20 ml samples from each chamber at four time points every 10 min. The replicate chambers were pooled in one pre-evacuated glass serum bottle (20 ml volume) after flushing, resulting in over-pressurized vials. (Butterbach-Bahl et al., 2016; Clough et al., 2020; Parkin & Venterea, 2010). The filled gas vials were stored at room temperature for a maximum of one week and then analyzed for CO_2, CH_4, and N_2O concentrations at the Mazingira Center of the International Livestock Research Institute, Nairobi, using a GC-ECD/FID system (GC; SRI Instruments, USA model 8610 C). For the portable LI-COR analyzers (last four sampling campaigns), one chamber lid was modified and fitted with two transparent 2 m-long tubes, one on the gas sampling point of the chamber lid and the other on the opposite side of the sampling point to facilitate air circulation. The tubes were connected to the appropriate inlet and outlet points of the LI-COR instrument. Gas concentrations were obtained by placing the chamber lid on top of the chamber base and closing it tightly using fold-back binder clips for 5 min, after which the chamber lid was removed and gently waved to restore the air concentrations inside the chamber to ambient baseline levels. Once the ambient levels were attained, another gas measurement was taken on the next chamber.

2.4.2 Soil GHG analysis and calculation

The gas samples were analyzed for GHG concentrations (CO_2, CH_4, and N_2O). The GHG fluxes were then calculated using linear regression, based on the slope of the concentrations over the deployment time (Butterbach-Bahl et al., 2011; Venterea et al., 2009; Equation 1).

$$\boldsymbol{Gas\ flux} = \frac{C_v \times MW \times slope}{C_A \times V_m} \times 60 \times 10^3 \qquad (1a)$$

$$\boldsymbol{V_m} = 0.02241 \times \frac{273.1 + temp}{273.1} \times \frac{P_{atm}}{P_0} \qquad (1b)$$

Where Gas flux is the GHG flux (1a; mg CO_2-C m^{-2} h^{-1}, mg CH_4-C m^{-2} h^{-1}, µg N_2O -N m^{-2} h^{-1}), C_V is the chamber volume (m^3), MW is the molar mass ($gmol^{-1}$) of carbon (12 for CH_4 and CO_2) or nitrogen ($2 \times 14 = 28$ for N_2O), slope is the rate of change in gas concentration over time ($ppmv\ min^{-1}$), C_A is the chamber area (m^2), 60 is a time conversion factor from minutes to hours, and 10^3 converts mass from g to mg. V_m (1b) is the molar volume (m^3mol^{-1}) which is further corrected for air pressure and temperature, temp is the headspace air temperature (°C). P_{atm} is the atmospheric pressure at the site, and P_0 is the atmospheric pressure at sea level.

The quality of the flux data was based on the R^2 value of the linear slope of the gas concentration over time, where the flux was accepted when R^2 was ≥ 0.9 for CO_2. In cases where the CO_2 R^2 was < 0.9, the measurement was assumed to be faulty (e.g., leaky chamber or vial), and the fluxes of all three GHGs were excluded. In addition, negative CO_2 fluxes were discarded along with all other gases, assuming faulty measurements, whereas negative fluxes for CH_4 and N_2O were retained and interpreted as gas uptake, potentially as either methane oxidation (Ueyama et al., 2021), or conversion of atmospheric N_2O to N_2 through total denitrification (Liu et al., 2022). In cases where the gas concentrations at the first chamber time point (T0) were significantly higher than the ambient concentrations, fluxes were discarded because they violated the assumption of a known baseline. In situations where the R^2 values for CH_4 and N_2O were low (< 0.7), and the concentrations indicated very low or no change, these results were included to avoid over- or underestimation of fluxes. Results from the LI-COR CH_4 scatter plots indicating ebullition at the start of the measurements were analyzed, and some were eliminated from the calculation to avoid overestimation. In total, this led to the exclusion of 1% of CO_2, 6% of CH_4, and 4% of N_2O data points.

The LI-COR instruments were used to measure gas concentrations in each static chamber for five minutes, with the start time recorded immediately after chamber closure and the end time after five minutes. Flux calculations for the LI-COR measurements were performed using the goFlux package in R (R Core Team, 2024; Rheault et al., 2024).

2.4.3 Cumulative emissions

The gas fluxes were aggregated into biweekly mean values with associated standard errors across each wetland type at all study sites. The cumulative emissions over one year were calculated using the trapezoidal integration method, which involves linear interpolation to fill in gaps and numerical integration between sampling times using the "Approxfun" function in R-studio (Keane et al., 2018; Minamikawa et al., 2015). To account for uncertainty, the standard errors of the biweekly fluxes

were propagated using the trapezoidal rule, which incorporates the variance and the covariance between each interval to account for overlap. This yields not only the cumulative emissions for each wetland but also their confidence intervals.

2.4.3 Soil sampling and analysis

In-situ soil moisture and soil temperature were measured in each chamber using ProCheck RS 232 soil sensors to a depth of 3 cm. Because these sensors are not always accurate for saturated soil, we also collected soil samples for gravimetric determination of moisture content at each site. Composite samples (10 cm depth) from three different locations at each site were collected to determine mineral N (NH_4-N and NO_3-N), soil organic carbon concentration (SOC), and total nitrogen (TN). Soil bulk density (BD) samples were collected using a core ring of known volume alongside samples for SOC concentration analysis. Both SOC and BD were collected at depths of 0-10, 10-20, 20-30, 40-50, and 50-60 cm to assess SOC stocks across different wetlands and to elevated changes in BD. SOC was calculated from the bulk density and SOC concentration, considering the soil depth at which the sample was collected, as described in Equation 2 (Ellert et al., 2007). Wetland conversion alters soil bulk density, which can bias SOC stock calculations when based on fixed depths (Fowler et al., 2023; Rovira et al., 2022; von Haden et al., 2020). Therefore, SOC stocks were corrected using the equivalent soil mass approach to improve the accuracy of comparisons to adjust for the fixed depth error (Fowler et al., 2023; Rovira et al., 2022; von Haden et al., 2020; Equation 3). The core assumption was that soil mass remained relatively constant across the different sampling periods. The intact HVBW was used as the reference site for the equivalent soil mass correction.

$$SOC_{FD} = BD \times \%C \times sd \times 0.1 \qquad (2)$$

where SOC_{FD} is the soil organic carbon stock at a fixed depth (Mg C ha^{-1}), BD is the bulk density (g cm^{-3}), %C is the percentage of carbon measured in the laboratory, converted into mg g^{-1} using the 0.1 factor, and sd is the soil depth segment (cm).

$$SOC_{FM} = SOC_{FD} - M_{ex} \times (\%C \div 100) \quad (3)$$

where SOC_{FM} is the SOC stock for a fixed mass, M_{ex} is the excess calculated from the deepest depth, and %C is the SOC concentration in the deepest soil core segment (conversion factor 100).

Mineral N (NH_4-N and NO_3-N) was measured from extracts of fresh soil (approximately 4 g), which were shaken with 20 mL of 1 M KCl solution, corresponding to an approximate solution-to-dry-soil ratio of 1:5 (w/v), and measured using colorimetric methods on a microplate reader (BioTek Synergy LX Multi-Mode Microplate Reader; Vermont, USA). NO_3-N was measured after oxidation using vanadium chloride (VCL_3) and colorimetric determination through an acidic reaction using Griess reagents, while NH_4-N was measured using the Berthelot colorimetric reaction (Hood-Nowotny et al., 2010; Wangari et al., 2022). Soil water content (WC) and BD were determined using fresh soil samples by oven-drying at 105°C until constant weights was achieved. Soil SOC and TN were analyzed on samples dried at 50°C using an elemental analyzer (VarioMAX Cube elemental analyzer, Elementar GmbH, Hanau, Germany). The pH was measured on air-dried samples in distilled water extracts (1:2.5 soil-water mix ratio) using a pH electrode (JENWAY 3540, Cole Parmer, UK).

2.3 Statistical data analysis

Gas fluxes were subjected to normality testing using histograms, QQ plots, and the Shapiro-Wilk test. In general, most variables violated the assumption of normality, and we therefore used a combination of non-parametric tests (Kruskal-Wallis tests and Kendall tests) and log transformation for statistical comparisons and tests. Non-normally distributed data were log-transformed to approximate normality prior to use in linear mixed effects models (LMM). Kruskal-Wallis tests were used to assess the influence of wetland type on soil site characteristics (%C, %N, C:N ratio, SOC, bulk density, and soil pH) and that of wetland type and season on GHG fluxes and dynamic soil variable (NO_3-N, NH_4-N, soil moisture, and soil temperature). The results were then subjected to Dunn's post hoc analysis to identify significant differences ($p < 0.05$) between wetland types and seasons. The Kendall test was used to test for correlations among GHG fluxes and soil variables, as well as among the variables themselves.

To identify potential controlling factors for different GHG fluxes, we used LMM specifically the nlme package in R with variance structures (Pinheiro et al., 2026). We systematically tested different predictor models based on proximate (e.g., soil moisture, C, N, and temperature) and distal (e.g., wetland type) controls for each gas. Predictor variables were tested for collinearity and were not included in the same model when the correlation coefficients were above 0.5. Following the procedure of Zuur et al. (2007) and Zuur & Ieno (2016), we first developed a model with a high R^2 without including random effects or variance structure and tested model improvements based on Akaike's information criterion (AIC), Bayesian information criterion (BIC), and the normality of residuals. The best-fitting models included sampling site as a random effect (random intercept) and a variance structure (implemented using the varIdent function) for each site to account for heteroscedasticity. All statistical analyses were performed using R-Studio software version 4.2.1 (R Core Team, 2024). Unless explicitly stated otherwise, the results are shown as mean ± standard error ($\bar{x}$ ± SE), and only statistically significant differences are reported.

3 Results

3.1 Climatic conditions

Over the study period, total rainfall in the study area was 1388 mm over 16 months (November 2022 to April 2024; Figure S7). The long rains from mid-March to May 2023 totalled 366 mm, with April contributing 53% of the seasonal rainfall, while the short rains from mid-October to mid-December totalled 112 mm in 2022 and 614 mm in 2023, with November contributing the highest proportion in both years (> 80%). The long dry season from June to September 2023 had a total rainfall of 63 mm. The mean monthly temperatures ranged from 16 ± 0.1 °C to 20 ± 0.1 °C. The wet seasons were cooler than the dry seasons, with a mean monthly air temperature of 19 ± 0.1 °C during the wet season compared with 18 ± 0.3 °C during the dry season.

3.2 Soil characteristics

The soil characteristics in the top 0 – 10 cm varied among the HVBW types (Figure 2). The intact HVBWs had the highest mean SOC concentration (5.2 ± 0.7%), which was statistically different from the recovering (4.6 ± 0.5%) and converted (3.2 ± 0.3%) HVBWs (Figure 2A). TN concentration was also highest in the intact HVBW (0.4 ± 0.1%) and lowest in the converted HVBW (0.25 ± 0.02%; Figure 2B). The soil C:N ratios were 15.9 ± 0.5 for the recovering, 13.8 ± 0.03 for the intact, and 14.4 ± 0.3 for converted HVBWs (Figure 2C). Soil C/NO_3^--N was significantly different across HVBW types, with the intact HVBW showing the highest ratio compared to the converted HVBW with the lowest, and the recovering HVBW intermediate (Figure 2D).

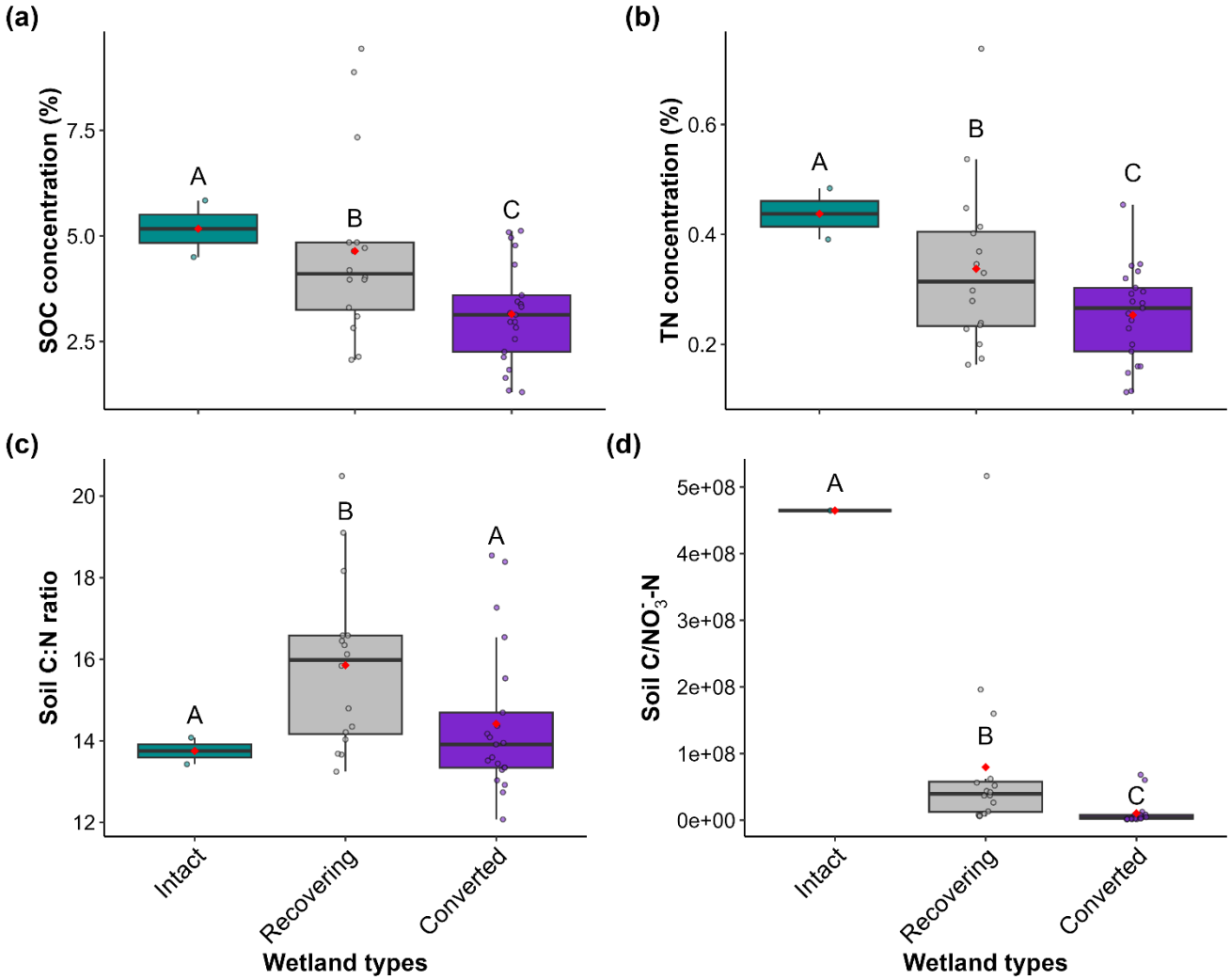

Figure 2: *Box plots showing soil characteristics in the upper 0 -10 cm of the sites in different Highland Valley-Bottom Wetland (HVBW) types. Intact refers to HVBWs that have never been used for agriculture (n = 1.; recovering refers to HVBWs previously converted to croplands but subsequently abandoned (n = 09); and converted refers to drained wetlands currently used for crop production (n = 11). Two sites (Munuka, converted, and Ngelenyi, recovering) were removed from the dataset as they were both above the 99th percentile (z-score=2.9). Uppercase letters indicate significant differences between wetland types based on Dunn's post-hoc test (p<0.05) following the Kruskal-Wallis test.* SOC refers to soil organic carbon, *and TN refers to total soil nitrogen. The soil C:N ratio and the C/NO_3^-–N ratio were calculated on a molar basis. The boxes represent the interquartile range (25th and 75th percentiles), and the whiskers extend to 1.5 times the interquartile range (IQR). The horizontal line indicates the median, and the red point represents the mean. Points inside and around the box and whiskers represent data spread, while those above and below the whiskers represent outliers.*

Soil moisture, temperature, and nitrate (NO_3^--N) and ammonium (NH_4^+–N) concentrations in the upper 10 cm varied across wetland types and seasons (Figures 3A, 3B, 3C, and 3D). Overall, the converted HVBWs exhibited significantly lower soil moisture and higher soil temperatures than the recovering and intact HVBWs, with patterns varying seasonally. Specifically, soil moisture in the converted HVBWs was significantly different from that in the recovering and the intact HVBWs, with 28.5 ± 0.5%, which was 1.8 times lower than recovering (52.5 ± 0.9 %) and 1.5 times lower than intact HVBWs (45.0 ± 1.8%; Figure S6). Also, seasonally, soil moisture in converted wetlands was always lower than in recovering and intact HVBWs per season (Figure 3). Both converted and recovering HVBWs had significantly lower NH_4^+–N concentrations (6.3 ± 0.3 µg NH_4^+–N g^{-1} (dry weight) DW and 18.6 ± 1.3 µg NH_4^+–N g^{-1} DW, respectively) than in the intact HVBWs, which exhibited approximately eight-fold higher NH_4^+–N concentrations (47.4 ± 5.8 µg g^{-1} DW; Figure S6). Similarly, seasonal NH_4^+–N concentrations were always lower in the converted and recovering wetlands than in the intact wetlands (Figure 3D). In contrast, the converted HVBWs had the highest NO_3^--N concentrations (14.3 ± 0.9 µg NO_3^--N g^{-1} DW), whereas the intact and recovering wetlands showed substantially lower NO_3^--N concentrations (0.6 ± 0.1 µg NO_3^--N g^{-1} DW and 1.9 ± 0.2 µg NO_3^--N g^{-1} DW, respectively; Figure S6). This trend was also evident across seasons (Figure 3C). The recovering HVBWs showed seasonal variation in soil temperature (with higher values during the dry seasons and lower values during the wet seasons), whereas they were not significantly different in all cases (moisture, temperature, NO_3^--N, and NH_4^+-N; Figure 3).

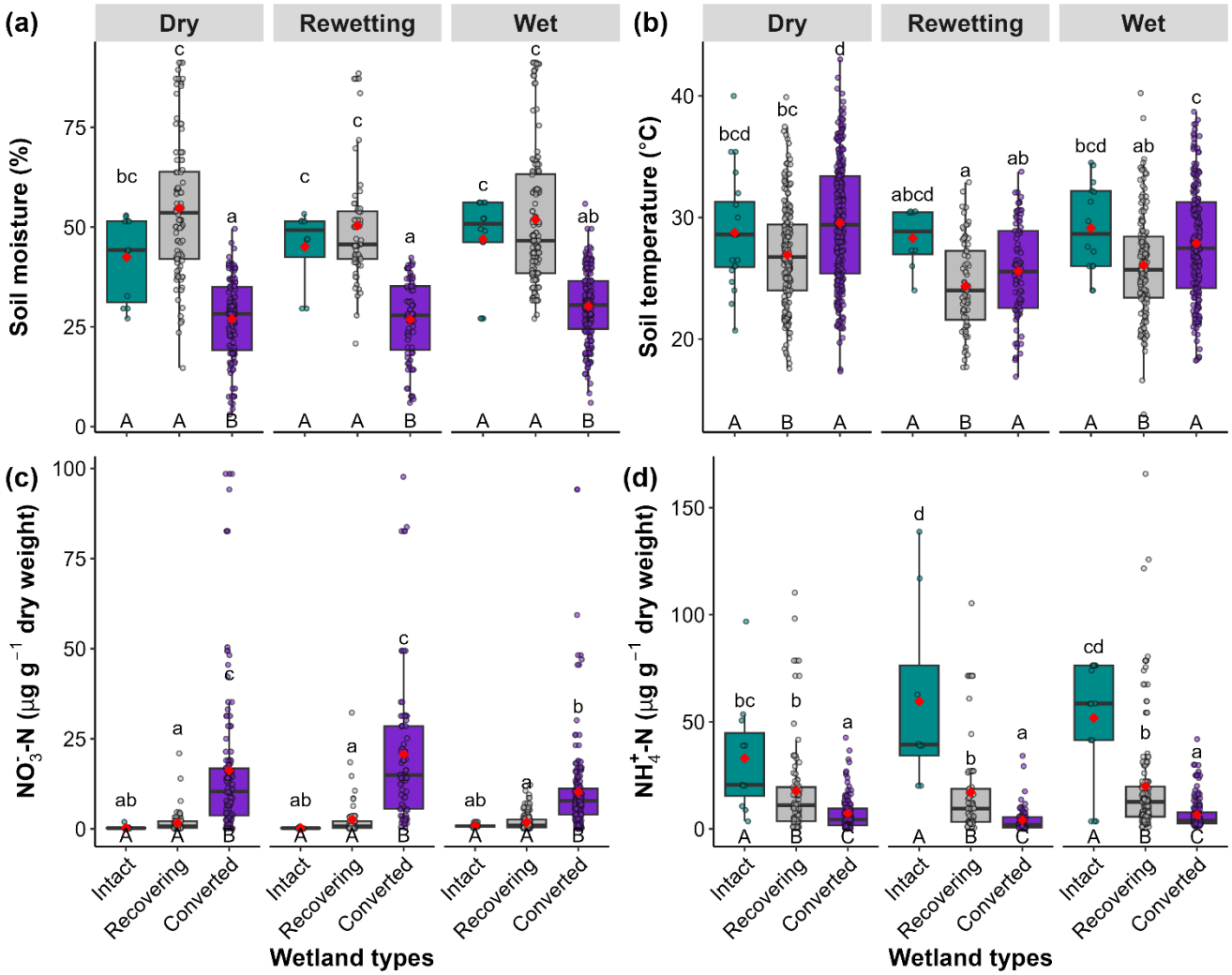

Figure 3: *Boxplots showing soil characteristics in the different Highland Valley-Bottom Wetland (HVBW) types and seasons (dry season: January to mid-March 2024 and June to September 2023; wet season: mid-March to May 2023 and mid-October to mid-December 2023). Rewetting fluxes were defined as measurements collected following a dry period of at least 10 consecutive days without rainfall, as well as measurements collected following the first rainfall event marking the onset of the rainy season. Together, these measurements represented rewetting conditions observed both within the dry season and during the transition from the dry to the wet season (20 days in total). Intact refers to HVBWs that have never been used for agriculture (n = 1); recovering refers to HVBWs previously converted to croplands but subsequently abandoned (n = 10); and converted refers to drained wetlands currently used for crop production (n = 12). Soil moisture (%) was determined gravimetrically. Uppercase letters indicate significant differences ($p < 0.05$) between wetland types, whereas lowercase letters indicate*

significant differences between seasons for each wetland type (Dunn's post hoc test; $p < 0.05$). NO_3^- and NH_4^+ represent nitrate and ammonium, respectively.

3.3 Soil organic carbon stocks

Integrated over the sampled depth profile (0 – 60 cm), the intact HVBW had the highest SOC stock (224.27 Mg C ha^{-1}) with the lowest average bulk density (BD; 0.6 ± 0.06 g cm-3) (Figures 4A & 4B). In contrast, the converted HVBWs showed the lowest SOC stocks of 103.25 ± 17 Mg C ha^{-1} (0 – 60 cm) and the highest average BD (1.1 ± 0.04 g cm-3). The recovering HVBWs had intermediate SOC stocks (143.16 ± 22 Mg C ha^{-1}) and BD (0.9 ± 0.04 g cm-3).

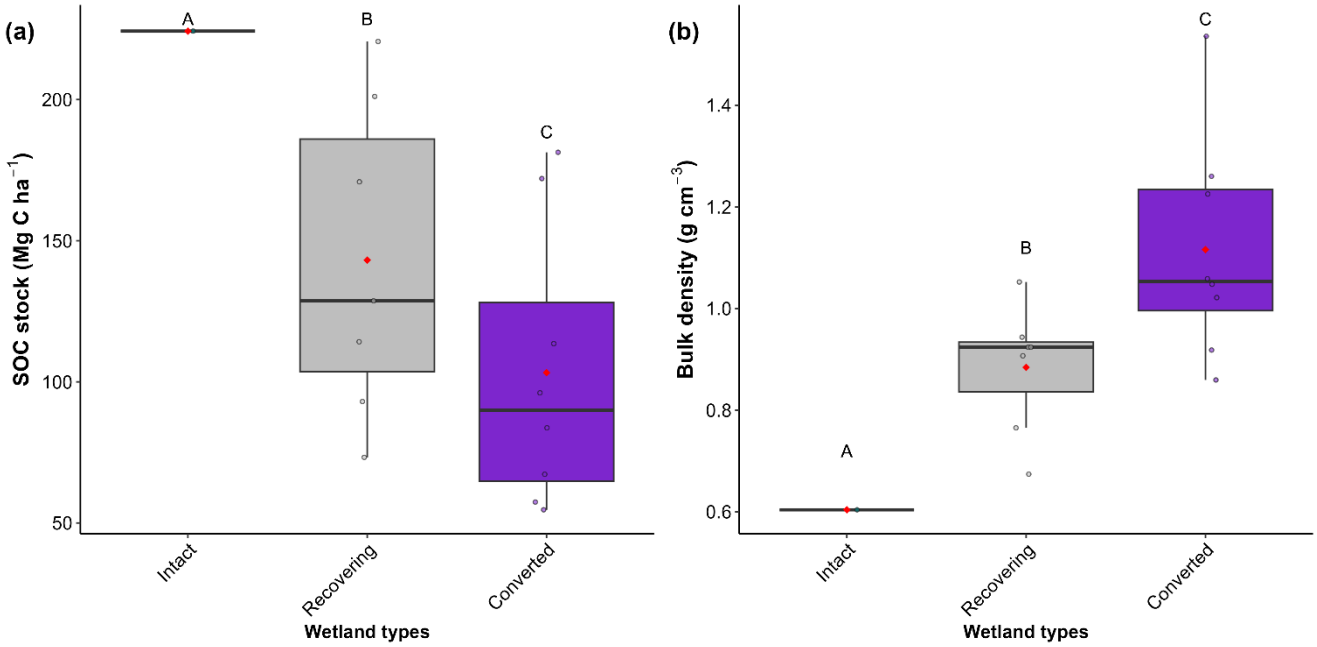

Figure 4: *Bar plots with error bars showing SOC stocks (A) and bulk density (B) by depth (0 – 60 cm) for each Highland Valley-Bottom Wetland (HVBW) type. Intact refers to HVBWs that have never been used for agriculture (n = 1); recovering refers to HVBWs previously converted to croplands but subsequently abandoned (n = 10); and converted refers to drained wetlands currently used for crop production (n = 12).*

3.2 GHG fluxes

3.4.1 Nitrous oxide (N_2O - N) flux rates

Over the entire sampling period, N_2O-N fluxes across all sites ranged from -38.88 to 585.75 (µg m^{-2} h^{-1}) with a coefficient of variation (Cv) of 3.1% (Table S2). N_2O-N fluxes were highest in the converted HVBWs (30.97 ± 3.13 µg N_2O-N m^{-2} h^{-1}), intermediate in the recovering HVBWs (5.47 ± 1.08 µg N_2O-N m^{-2} h^{-1}), and negative in the intact HVBW (-3.83 ± 1.67 µg

N_2O-N m^{-2} h^{-1}), indicating net N_2O uptake (Figure 5A; Figure S5; Table S2). There were no significant differences in the intact HVBWs by season. However, the recovering HVBWs had lower fluxes in the dry season (3.01 ± 1.20 µg N_2O-N m^{-2} h^{-1}) compared to the rewetting events (5.02 ± 4.22 µg N_2O-N m^{-2} h^{-1}) and higher fluxes in the wet season (9.05 ± 1.81 µg N_2O-N m^{-2} h^{-1}; Figure 5A; Dunn's post-hoc $p < 0.05$). The converted HVBWs also exhibited significantly lower fluxes during the dry season than during the wet season. The converted HVBWs exhibited higher mean fluxes during rewetting events (73.9 ± 16 µg N_2O-N m^{-2} h^{-1}), similar to the intact HVBWs (-1.94 ± 2.1 µg N_2O-N m^{-2} h^{-1}; Figure 5A).

3.4.2 Methane (CH_4-C) flux rates

CH_4-C fluxes ranged from -7.27 to 91.28 (mg CH_4-C m^{-2} h^{-1}) with a C_V of 2.3% (Table S2). Converted HVBWS had the lowest average CH_4 fluxes (0.48 ± 0.11 mg CH_4-C m^{-2} h^{-1}) and differed from intact (31.30 ± 5.45 mg CH_4-C m^{-2} h^{-1}) and recovering (10.45 ± 0.73 mg CH_4-C m^{-2} h^{-1}) wetlands (Figure 5B, Table S2). In general, the converted HVBWs exhibited near-zero CH_4 fluxes during most sampling campaigns. CH_4 fluxes were only significantly different across seasons in the converted HVBWs, with lower fluxes in the rewetting events (0.35 ± 0.13) being significant different from the intermediate fluxes during the wet season (0.45 ± 0.21) and the highest fluxes during the dry season (0.54 ± 0.16).

3.4.3 Carbon dioxide (CO_2 - C) flux rates

CO_2-C fluxes ranged from 2.73 to 530.99 (mg CO_2-C m^{-2} h^{-1}) with a C_V of 0.55 (Table S2). Overall, converted HVBWs had the highest mean CO_2 flux (137.61 ± 2.72 mg CO_2-C m^{-2} h^{-1}) across all seasons, closely followed by recovering HVBWs (134.01 ± 3.64 mg CO_2-C m^{-2} h^{-1}), whereas the mean CO_2 flux of intact HVBWs was two-fold lower (42.79 ± 5.11 mg CO_2-C m^{-2} h^{-1}; Figure 5C, Table S2). CO_2 fluxes were only significantly different in the recovering HVBWs, with the highest fluxes occurring during the dry season, whereas no significant seasonal differences were observed in the intact and converted HVBWs.

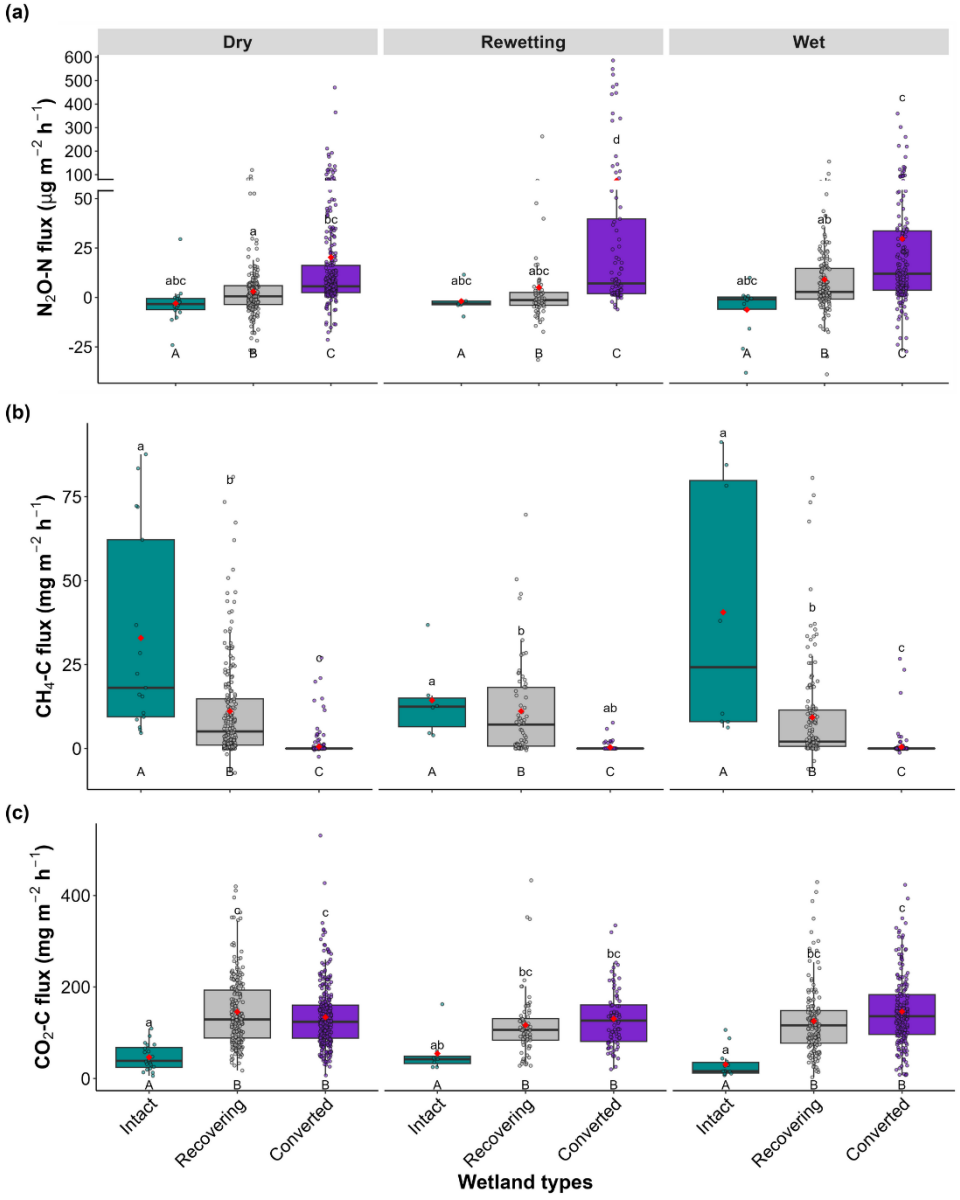

370 ***Figure 5:*** *Boxplots showing greenhouse gas fluxes from intact, recovering and converted Highland Valley-Bottom Wetlands (HVBW) across dry, rewetting and wet seasons. Uppercase letters indicate significant differences ($p < 0.05$) between wetland types, whereas lowercase letters indicate significant differences between seasons for each wetland type (Dunn's post hoc test; $p < 0.05$). The N_2O-N flux scale was split into two to accommodate very high flux values and improve the visibility of the lower fluxes. N_2O, CO_2, and CH_4 represent nitrous oxide, carbon dioxide, and methane, respectively.*

3.5 Cumulative emissions

Cumulative GHG emissions were calculated over one year (May 2023 to April 2024) for all three HVBW types (Figure 6; Table S8). The N_2O-N and CH_4-C fluxes showed opposite trends in the intact and converted HVBWs. Converted wetlands had the highest total emissions of N_2O (1.6 ± 0.2 kg N_2O-N ha^{-1}) and the lowest CH_4-C emissions (37.7 ± 9 kg CH_4-C ha^{-1}). In contrast, intact wetlands acted as a sink for N_2O (-0.3 ± 0.1 kg N_2O-N ha^{-1}) and had high CH_4 emissions (2757 ± 391 kg CH_4-C ha^{-1}). Recovering wetlands were intermediate for both gases (0.5 ± 0.1 kg N_2O-N ha^{-1} and 781 ± 65 kg CH_4-C ha^{-1}). With respect to CO_2, emissions from converted and recovering HVBWs were similar (9534 ± 239 kg CO_2-C ha^{-1} and 9610 ± 300 kg CO_2-C ha^{-1}, respectively) and were approximately threefold higher than those from the intact HVBW (2923 ± 214 kg CO_2-C ha^{-1}). Seasonal trends were evident, particularly for N_2O, where the rate of increase was higher during the wet season in converted wetlands (Figure 6). The rate of increase in CO_2 emissions in recovering wetlands decreased, as observed in the intact wetlands.

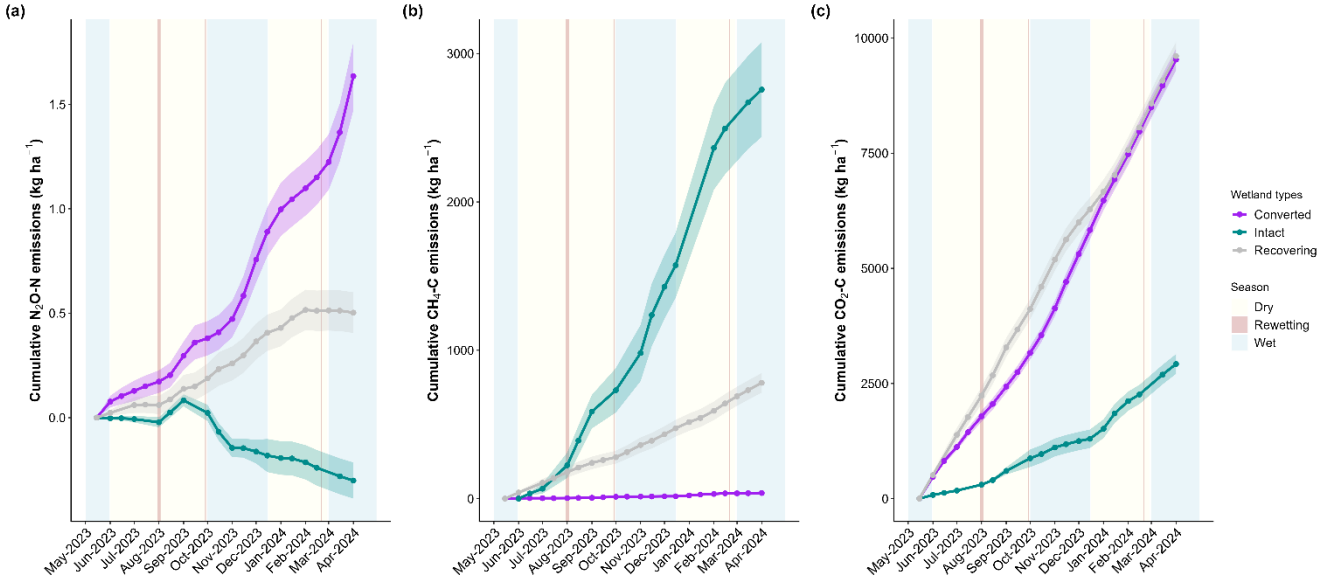

Figure 6: *Annual (May 2023 - April 2024) cumulative emissions of N_2O-N (Panel A), CH_4-C (Panel B) and CO_2-C (Panel C) based on trapezoidal integration of fortnightly measurements in converted HVBWs (n = 12), recovering Highland Valley-Bottom Wetlands (n = 10) and the intact wetland (n = 1). Blue shaded regions indicate wet seasons. N_2O, CO_2, and CH_4 represent nitrous oxide, carbon dioxide, and methane, respectively.*

3.6 Biogeochemical controls

The linear mixed-effects models (LMM) indicated that a combination of distal factors (wetland type and season) and proximate factors (soil characteristics) best described the different flux rates (Table 1). For N_2O-N flux, our best-fit model explained 29% of the variation (conditional R^2 (Nakagawa & Schielzeth, 2013), Table 1) and identified significant effects of wetland type,

395 NO_3^--N concentration, and season. Consistent with the non-parametric analysis shown in Figure 5, intact and recovering HVBWs showed significantly lower N_2O fluxes than converted HVBWs, and fluxes were significantly higher during the wet season ($p<0.001$; Table 1). Increasing NO_3 concentrations led to higher N_2O-N fluxes (positive slope, $p<0.0001$; Table 1). Rewetting events had a significant effect on recovering HVBWs, where N_2O-N fluxes were lower during these events (Table 1; Figure 5). Including soil carbon and nitrogen content and soil moisture did not improve model performance.

400 The LMM model for CH_4-C explained 75% of the variation (conditional R^2, Table 1) based on soil moisture and wetland type. Consistent with the non-parametric tests (Figure 5), CH_4 was higher in intact and recovering HVBWs (Table 1) and positively related to soil moisture across all sites. For CO_2-C, soil temperature and wetland type were included in the best-fit model but explained only 35% of the variation (conditional R^2; Table 1). Increasing soil temperature led to higher CO_2-C emissions, although CO_2-C emissions remained lower in intact wetlands than in converted and recovering wetlands (Table 2). Intact

405 HVBWs had lower CO_2-C flux rates than converted HVBWs.

Table 1: Best-fit linear-mixed models developed for each greenhouse gas. B indicates the model coefficients, with the intercept representing the reference variable of either converted wetlands (for CH_4 and CO_2) or converted wetlands during the dry season (N_2O). Significance levels are denoted as follows '***' $p < 0.001$, '**' $p < 0.01$,'*' $p < 0.05$, ms $p = 0.05$ (marginally significant), and ns $p > 0.05$ (not significant). The conditional R^2 values are also shown.

Predictor variables	**B**	**Standard error**	**p-values**
N_2O-N flux ($\mu g\ m^{-2}\ h^{-1}$)			
Intercept	1.51	0.24	***
NO_3^--N (µg g-1 DW)	0.03	0.006	***
Wetland type (intact)	-2.35	0.70	***
Wetland type (recovering)	-0.94	0.27	***
Season (rewetting events)	0.46	0.25	ns
Season (wet)	0.61	0.21	**
Wetland type (intact) x Season (rewetting events)	-0.59	0.94	ns
Wetland type (recovering) x Season (rewetting events)	-1.16	0.39	**
Wetland type (intact) x Season (wet)	-0.69	0.83	ns
Wetland type (recovering) x Season (wet)	-1.17	0.31	ns
R^2	0.29		
CH_4-C flux ($mg\ m^{-2}\ h^{-1}$)			
Intercept	-0.24	0.13	*
Soil moisture (%)	0.01	0.003	***
Wetland type (intact)	2.59	0.185	***

Wetland type (recovering)	1.06	0.087	***
R^2	0.74		
CO_2-C flux (mg m^{-2} h^{-1})			
Intercept	4.24	0.13	***
Soil temperature (°C)	0.02	0.004	***
Wetland type (intact)	-1.18	0.14	***
Wetland type (recovering)	-0.003	0.039	ns
R^2	0.33		

4 Discussion

4.1 Overview of GHG flux patterns across wetland types

Overall, GHG emissions varied significantly across intact, recovering, and converted HVBWs, highlighting the strong impact of land use practices and history, as well as hydrological changes on wetland biogeochemistry. The intact HVBW was characterized by CH_4-C emissions that were more than two orders of magnitude higher than those of the converted wetlands, but approximately two orders of magnitude lower CO_2-C fluxes, and it acted as a sink for N_2O-N. In contrast, the converted HVBWs showed the opposite trend, with significantly higher N_2O-N and CO_2-C emissions and minimal or negative CH_4 fluxes. The recovering HVBWs showed intermediate fluxes for all gases, suggesting partial recovery of hydrological conditions and microbial functions (Kluber et al., 2014). The shift from CH_4-dominated to N_2O-dominated emissions, along with other emission changes in the investigated sites, aligns with the results from a global meta-analysis (Tan et al., 2020) and other field-scale studies in northern regions (Berglund et al., 2021; L. Li et al., 2025; F. Liu et al., 2025). Although studies from African wetlands are rare, these results are consistent with patterns found in a lowland, *Cyperus papyrus*-dominated wetland in Kenya under small-scale farming (Ondiek et al., 2021).

The GHG emissions measured in this study are within the range reported for other chamber-based flux measurements in both intact and converted wetlands in Africa (Table 2). Although few studies exist on GHG emissions in these regions (Table 2), data from African wetlands show that N_2O-N emissions vary widely across wetland types, while CH_4 emissions are notably affected by soil moisture and water-table levels. When compared to fluxes reported for other African wetlands (Table 2), CH_4 emissions from the intact HVBW fall within the typical range of tropical peat and mineral wetlands, while N_2O fluxes in converted HVBWs were comparable to, but higher than, those reported from intensively cultivated Zimbabwean wetlands (Gondwe & Masamba, 2014; Nyamadzawo et al., 2015; Were et al., 2021). CO_2 fluxes were also within the range of both global and African wetland emissions, confirming that HVBWs significantly contribute to regional GHG budgets (Convention on Wetlands, 2025; Nyamadzawo et al., 2015; Schuster et al., 2024). As shown in Table 2, all African studies reporting seasonal

fluxes found no significant variation, which is comparable to our findings. In our study, seasonal variations only occurred in the recovering and converted HVBWs, and only for N_2O. Overall, these trends indicate that hydrology is a key regulator of GHG exchange, controlling the balance between aerobic decomposition, methanogenesis, and denitrification.

4.2 Nitrous oxide (N_2O) dynamics

Nitrous oxide fluxes varied significantly across different HVBW types, with converted HVBWs showing the highest emissions, recovering HVBWs showing intermediate levels, and the intact HVBW acting as a net N_2O sink. The LMM identified season, soil moisture, NO_3-N concentration, and wetland type as key predictors of N_2O fluxes, highlighting the strong connection between hydrology and nitrogen availability in wetlands.

Converted HVBWs had high concentrations of NO_3-N, indicating enhanced nitrification, thereby increasing N_2O dynamics and emissions (Ashiq et al., 2022; Bahram et al., 2022; Butterbach-Bahl et al., 2013). Agricultural intensification, including increased N inputs and drainage, increases soil aeration and microbial activity, thereby promoting N_2O production (Ashiq et al., 2022; Hatano, 2019). Although not statistically significant, rewetting events in the converted HVBWs showed higher mean N_2O fluxes, triggering short-lived but intense N_2O pulses, referred to as "hot moments," during which microbial communities rapidly transition between oxic and anoxic microsites (Berendt et al., 2023; Elberling et al., 2023). Continued aeration and land-use conversion in HVBWs accelerated organic matter decomposition by increasing oxygen availability and microbial respiration, thereby accelerating C conversion to CO_2. Wetland degradation and N inputs from fertilizers and manure further stimulated nitrification and N_2O emissions.

In contrast, the intact HVBW exhibited low to negative N_2O fluxes, consistent with low NO_3-N concentrations and persistently anaerobic conditions. These conditions likely promoted complete denitrification, enabling microbial reduction of N_2O to N_2 and resulting in net N_2O uptake rather than emission (Butterbach-Bahl et al., 2013; Martínez-Espinosa et al., 2021). Saturated pore spaces and redox gradients typical of wetland soils further facilitated the reduction of N_2O to inert N_2 (Mander et al., 2025; Martínez-Espinosa et al., 2021). The observation that intact tropical African wetlands can act as N_2O sinks is notable and rarely documented. A study in Congo is one of the few African studies that indicated naturally inundated wetlands as N_2O sinks with negative fluxes of -0.19 kg N_2O-N ha^{-1} yr^{-1} (Barthel et al., 2022). Soil C is a key control on microbial processes in intact HVBWs. The comparatively high C/ NO_3^--N ratio in the intact HVBW promotes complete denitrification by providing sufficient organic carbon as an electron donor relative to NO_3^- availability (Allen et al., 2023).

Recovering HVBWs showed intermediate N_2O emissions, reflecting partial hydrological recovery and transitional nitrogen dynamics. Legacy effects of past cultivation and fertilizer use likely promoted incomplete denitrification, leading to variable N_2O emissions. Emissions decreased during rewetting periods, causing these wetlands behave more like intact systems. Intermediate C and NO_3^--N levels suggest that carbon availability was insufficient for complete denitrification, resulting in N_2O release (Grebliunas & Perry, 2016).

Globally, natural and agricultural soils emit 2.5-6.5 Tg N_2O-N yr^{-1} (Tian et al., 2011), and agricultural conversion continues to drive increases in N_2O emissions at regional scale (Ritchie et al., 2020). Our findings fit these global patterns, indicating

that conversion amplifies N_2O emissions, whereas rewetting reduces emissions but does not immediately reverse them (Liu et al., 2019). This underscores the importance of hydrological management and reduced fertilizer input in mitigating N_2O losses during wetland restoration.

4.3 Methane (CH_4) dynamics

Methane fluxes showed the opposite trend to N_2O: the intact HVBW was a strong CH_4 source, recovering HVBWs were intermediate, and converted HVBWs acted as potential CH_4 sinks. The LMM identified soil moisture as the dominant control, with higher water tables likely promoting methanogenesis and drier soils favouring CH_4 oxidation. In intact HVBWs, persistent saturation (>50% soil moisture), high temperatures, and abundant organic carbon created favourable anaerobic conditions for methanogenic archaea, potentially resulting in higher CH_4 emissions (Jiang et al., 2025). High organic carbon availability further supported conditions for methanogenesis through methanogenic archaea (Ashiq et al., 2022; Bridgham et al., 2013; Mander et al., 2025; Shah et al., 2024). These fluxes were comparable to estimates for tropical wetland, where CH_4 emissions contribute 58–60% of the global wetland CH_4 output (Murguia-Flores et al., 2023; Poulter et al., 2017). According to Delwiche et al. (2021), global freshwater wetlands typically emit 0 - 200 kg C ha^{-1} yr^{-1}, with a few emitting 200 - 600 kg C ha^{-1} yr^{-1}. These ranges are much lower than the emissions from the Taita Hills (On average 37 - 2,757 kg CH_4-C ha^{-1} yr^{-1}).

The recovering HVBWs emitted high CH_4 levels, reflecting the partial restoration of anaerobic conditions. This suggests that hydrological recovery can rapidly re-establish the CH_4 production potential, even though microbial communities may take longer to fully re-establish (Schuster et al., 2025). The much lower CH_4 emissions observed in some recovering HVBWs compared to intact HVBWs might reflect altered microbial communities, vegetation differences and delayed re-establishment of favourable biogeochemical conditions in recovering wetlands (Antonijević et al., 2025). In contrast, the converted HVBWs exhibited near-zero or negative CH_4 fluxes, indicating net CH_4 uptake driven by methane oxidizers under aerobic conditions with low soil moisture. Drier soils (25–35% moisture) inhibit methanogenesis but enhance CH_4 oxidation (Le Mer & Roger, 2001; Wagner, 2017). Fertilizer-derived nitrogen may also suppress CH_4 uptake by increasing microbial growth (Wangari et al., 2022; Wu et al., 2021), thereby compounding these effects. Thus, CH_4 dynamics in HVBWs are primarily governed by soil moisture and the associated redox potential, with conversion and drainage strongly reducing CH_4 emissions but at the cost of increased N_2O and CO_2 fluxes.

4.4 Carbon dioxide (CO_2) dynamics

Overall, CO_2 emissions cumulatively increased over time across all three HVBWs. CO_2 fluxes also varied across wetland types, with the highest emissions in converted HVBWs. The CO_2 flux ranges recorded in the agricultural wetlands in Sweden (43 – 1661 mg C m^{-2} h^{-1}) were higher than those in Taita Hills HVBW (2.73 530.99 mg C m^{-2} h^{-1}). The LMM revealed that soil temperature and moisture were key predictors, emphasizing the roles of microbial respiration and decomposition under varying hydrological conditions.

In the converted HVBWs, annual CO_2 emissions were nearly double those from the intact HVBWs, which is consistent with rapid organic matter mineralization following drainage and cultivation. Aeration enhances the microbial oxidation of organic carbon, whereas tillage and root respiration further contribute to CO_2 emissions (Batson et al., 2015; Hao et al., 2025). Elevated soil temperatures and higher bulk density in converted HVBWs were associated with increased organic matter decomposition (Ndah et al., 2024), lower SOC stocks, and higher CO_2 emissions (Tangen & Bansal, 2020).

The recovering HVBWs displayed intermediate fluxes, reflecting partial restoration of water table conditions and microbial processes. Seasonal patterns were less pronounced for N_2O, suggesting more continuous respiration across the moisture regimes. The decomposition of legacy carbon is likely responsible for the elevated CO_2 release, even under improved hydrological conditions (McDaniel et al., 2019).

4.5 Soil organic carbon

Wetland conversion also corresponded to a reduction in C and N concentrations and stocks, which is consistent with global trends (Tan et al., 2022). Lower SOC stocks in converted HVBWs compared to intact and recovering sites reflect soil degradation due to land use conversion. Similar to other studies, long-term cultivation, drainage, and soil compaction enhance organic matter decomposition, elevating GHG emissions and bulk density, while reducing SOC stocks (Itoh et al., 2017; Prananto et al., 2020; Xu et al., 2019). Intact and recovering HVBWs exhibited bulk densities typical of organic soils, whereas converted sites display compacted mineral characteristics and enhanced CO_2 release from microbial activity under warmer and drier conditions (FAO, 2023; Tangen & Bansal, 2020). These findings are consistent with global evidence that agricultural conversion increases emissions while depleting soil carbon stocks (Beillouin et al., 2023; Li et al., 2025).

SOC patterns also indicated partial recovery in restored systems. Recovering HVBWs accumulated more SOC in surface layers (0–30 cm) than converted HVBWs but remained lower than intact HVBWs at depth (30–60 cm), reflecting slower subsurface recovery rates. This supports the finding that while GHG fluxes respond rapidly to restoration, full SOC recovery occurs over decades to centuries (Ascenzi et al., 2025; Tangen & Bansal, 2020). Intact HVBWs contained the highest stocks, maintaining high carbon sequestration despite elevated CH_4 emissions (Mitsch & Gosselink, 2015; Nahlik & Fennessy, 2016).

Differences in SOC stocks among intact, recovering, and converted HVBWs reflect both the magnitude of land-use impacts and the rate of recovery. Based on Gubamwoyo et al. (2025), the total HVBWs area in the Taita Hills is approximately 194 ha. Using the intact HVBW as a reference, the original SOC was 43,456 Mg C. Complete conversion to agriculture would reduce this to 19,982 Mg C, a loss of 23,474 Mg C. Assuming that most wetlands were converted 45 years ago (based on small holder interviews, Gubamwoyo et al., 2025), converted HVBW have a mean annual loss rate of 2.7 Mg C ha^{-1} yr^{-1}. Recovering HVBWs were abandoned ~35 years ago (Gubamwoyo et al., 2025), and assuming sequestration as the difference between the converted and the recovering stocks, the mean sequestration rate is 1.1 Mg C ha^{-1} yr^{-1}, although these stocks are currently 30% lower than in the intact HVBW. These rates fall within the global ranges reported for restored wetlands (0.5–3.0 Mg C ha^{-1} yr^{-1}; Abrar et al., 2025; Mitsch et al., 2013). However, these estimates should be interpreted with caution, as they assume linear loss rates. In fact, SOC accumulation is influenced by factors such as carbon litter quality, hydrological

stability, disturbance history, and environmental variability (Tangen & Bansal, 2020). Chronosequence analyses, characterization of carbon quality, and dating of soil cores would further refine these estimates. Nonetheless, abandoned wetlands exhibit encouraging SOC recovery and intermediate GHG emissions, suggesting gains from partially restoring these wetlands. Studies from rewetted freshwater mineral-soil wetlands indicate that organic carbon sequestration may transiently increase during the early post-rewetting phase before stabilizing over decadal timescales (Mistry et al., 2026). Assuming that 50% of the converted HVBWs in the Taita Hills are restored, it would result in 71.5 1 Mg C yr^{-1} sequestered, or roughly 0.0005% of Kenya's annual agricultural emissions, based on 2024 emission estimates (Climate Watch, 2025). Based on a wetland classification for HVBWs in Kenya (Gubamwoyo et al., 2025; Gubamwoyo et al., in prep), restoring 50% of HVBWs across Kenya could sequester up to 1.5 million Mg C yr^{-1}, representing up to 9.8% of the agricultural-based emissions.

4.6 Global Warming Potential

The Global Warming Potential (GWP; $CH_4 + N_2O + CO_2$) varied among all HVBW types, with the intact HVBW showing the highest values (77 Mg CO_2-eq ha^{-1} yr^{-1}), followed by recovering (35 Mg CO_2-eq ha^{-1} yr^{-1}) and converted HVBWs (13 Mg CO_2-eq ha^{-1} yr^{-1}). The high GWP in the intact HVBW was largely driven by CH_4 emissions associated with persistently anaerobic conditions, whereas conversion and drainage greatly reduced CH_4 fluxes, resulting in a lower overall GWP. Recovering wetlands showed intermediate values, reflecting partial re-establishment of hydrological conditions favoring CH_4 production.

Although intact HVBWs contribute substantially to global warming potential (GWP) owing to elevated CH_4 emissions, their large SOC stocks and low CO_2 fluxes make them long-term carbon sinks. Thus, despite serving as natural CH_4 sources, intact HVBWs maintain a positive carbon balance through persistent SOC sequestration. Globally, similar trends have been reported for natural wetlands with high CH_4 outputs alongside substantial carbon storage capacity (Ma et al., 2024; Mander et al., 2025). From a management perspective, protecting intact and recovering HVBWs is crucial for maintaining regional carbon balance and mitigating climate change impacts. Restoration targets under the Convention on Wetlands (2025), which aims to recover 30% of degraded wetlands, could effectively reduce CO_2 emissions. Complementary practices, such as maintaining high water tables and adopting low-input fertilizer strategies (Hochmuth et al., 2014), may further enhance mitigation outcomes in wetland-agriculture mosaics.

Table 2: Rates of GHG fluxes from African wetlands measured using the static chamber method. Ranges or means with standard errors are reported unless otherwise stated. Where season is not reported, an annual mean or range is used. Intact wetland fluxes represent measurements made under natural vegetation (NV) conditions. Agriculture codes are as follows: SHA = Smallholder agriculture (mixed crops), SHR = Smallholder Rice, SHP = Smallholder Potato, RB = Raised Beds, T = Trenches, NF = No fertilization, and SF = Standard Fertilization. (NOTE: The table was modified to fit on a portrait to meet submission requirements and header formatting, a landscape version is available)

Country	Location	Elevation (m. a. s. l.)	Site Description	Agricultural Use	Season	N_2O (µg N_2O-N m^{-2} h^{-1})		Reference
						Intact	Converted	
Kenya	Taita Hills 3.383°S, 38.362°E	800 - 1650	Riparian wetlands (Highland valley bottoms)	SHA	Dry	-1.5 ± 2	15.5 ± 2.3	This study
					Wet	-6.8 ± 2.7	28.6 ± 0.3	
Kenya	Anyiko Wetland 0.57°N, 38.56°E	1,465	Floodplain, Cyperus papyrus-dominated	SHR, NF	Annual		−3.59 ± 2.6	Owino et al. 2020
				SHR, NSF	Annual		4.37 ± 3.2	
Uganda	Naigombwa Wetland 1.05°N,33.41°E	1,045	Floodplain, Cyperus papyrus-dominated, with Typha latifolia and Phragmites mauritanus	SHR, NF	Dry	0.5 ± 1.5	0.6 ± 2.7	Were et al., 2021, 2023
					Wet	0.5 ± 1.5	0.7 ± 2.8	
	Ruhama Wetland, Kigezi Highlands - 1.208°N, 29.830°E	1930	Highland valley bottoms	SHP, RB	Dry			Farmer et al., 2022
					Wet			
				SHP, T	Dry			
					Wet			
Zimbabwe	Chiota 18.11°S, 31.05°E	1400	Dambo (stream bottom)	SHA	Wet		3.5 (-705 – 120)[b]	Nyamadzawo et al., 2015
			Dambo (mid slope)		Wet		2.5 (-60 – 80)[b]	
Democratic Republic of Congo	Mbandaka 0.063°N, 18.310°E	300	Seasonally Flooded Swamp Forest	NV	Annual	39.4 (21.1 – 72.4)[c]		Barthel et al., 2022; de Clippele et al., 2025
					Annual	-2.17 (-8.56 – 8.68)[c]		
Botswana 19°S to 20°S; 22°E to 24°E	Guma	930 - 1000	Floodplain	NV	Annual			Gondwe & Masamba, 2014
	Nxaraga				Annual			
	Xakanaxa				Annual			
	Okavango Delta				Annual			Gondwe et al., 2021
					Annual			
					Annual			
					Annual			

Table continued

Country	Location	Elevation (m. a. s. l.)	Site Description	Agricultural Use	Season	CH_4 (mg CH_4-C m^{-2} h^{-1})	Reference

						Intact	Converted	
Kenya	Taita Hills 3.383°S, 38.362°E	800 - 1650	Riparian wetlands (Highland valley bottoms)	SHA	Dry	29.2 ± 7	0.8 ± 0.2	This study
					Wet	33.9 ± 8.8	0.19 ± 0.1	
Kenya	Anyiko Wetland 0.57°N, 38.56°E	1,465	Floodplain, Cyperus papyrus-dominated	SHR, NF	Annual		8.3 ± 4.79	Owino et al. 2020
				SHR, NSF	Annual		4.00 ± 6.34	
Uganda	Naigombwa Wetland 1.05°N,33.41°E	1,045	Floodplain, Cyperus papyrus-dominated, with Typha latifolia and Phragmites mauritanus	SHR, NF	Dry	12.1 ± 0.8		Were et al., 2021, 2023
					Wet	16.3 ± 1.3		
	Ruhama Wetland, Kigezi Highlands - 1.208°N, 29.830°E	1930	Highland valley bottoms	SHP, RB	Dry			Farmer et al., 2022
					Wet			
				SHP, T	Dry			
					Wet			
Zimbabwe	Chiota 18.11°S, 31.05°E	1400	Dambo (stream bottom)	SHA	Wet		-0.98 (1.5 – 6.3)[b]	Nyamadzawo et al., 2015
			Dambo (mid slope)		Wet		22.1 (-8.5 – 84)[b]	
Democratic Republic of Congo	Mbandaka 0.063 °N, 18.310°E	300	Seasonally Flooded Swamp Forest	NV	Annual	0.03 (-0.04 – 0.14)[c]		Barthel et al., 2022; de Clippele et al., 2025
					Annual	3.89 (1.68 – 9.11)[c]		
Botswana 19°S to 20°S; 22°E to 24°E	Guma	930 - 1000	Floodplain	NV	Annual	17.4 ± 3.8[d]		Gondwe & Masamba, 2014
	Nxaraga				Annual	13.8 ± 2.7[d]		
	Xakanaxa				Annual	15.4 ± 3.6[d]		
	Okavango Delta				Annual	1.95 ± 0.5[d]		Gondwe et al., 2021
					Annual		-0.034 ± 0.004[d]	
					Annual			

Table continued

Country	**Location**	**Elevation (m. a. s. l.)**	**Site Description**	**Agricultural Use**	**Season**	**CO_2 (mg CO_2-C m^{-2} h^{-1})**		**Reference**
						Intact	Converted	
Kenya		800 - 1650		SHA	Dry	46.9 ± 8	123 ± 4.3	

	Taita Hills 3.383°S, 38.362°E		Riparian wetlands (Highland valley bottoms)		Wet	37.2 ± 5	42.3 ± 5	This study
Kenya	Anyiko Wetland 0.57°N, 38.56°E	1,465	Floodplain, Cyperus papyrus-dominated	SHR, NF	Annual		174.80 ± 26.8	Owino et al. 2020
				SHR, NSF	Annual		248.29 ± 41.2	
	Naigombwa Wetland 1.05°N,33.41°E	1,045	Floodplain, Cyperus papyrus-dominated, with Typha latifolia and Phragmites mauritanus	SHR, NF	Dry	788.1 ± 52.3		Were et al., 2021, 2023
					Wet	675 ± 52.7		
Uganda	Ruhama Wetland, Kigezi Highlands - 1.208°N, 29.830°E	1930	Highland valley bottoms	SHP, RB	Dry		273 ± 0.08[ad]	Farmer et al., 2022
					Wet		469 ± 0.19[ad]	
				SHP, T	Dry		0.06 ± 0.05[ad]	
Zimbabwe	Chiota 18.11°S, 31.05°E	1400	Dambo (stream bottom)	SHA	Wet		0.05 ± 0.03[a]	Nyamadzawo et al., 2015
					Wet		160.8 (-405 – 1595)[b]	
			Dambo (mid slope)		Wet		244 (-8.2-2612)[b]	
Democratic Republic of Congo	Mbandaka 0.063 °N, 18.310°E	300	Seasonally Flooded Swamp Forest	NV	Annual	102 ± 22[d] (37.6 – 157.23)[e]		Barthel et al., 2022; de Clippele et al., 2025
					Annual			
Botswana 19°S to 20°S; 22°E to 24°E	Guma	930 - 1000	Floodplain	NV	Annual			Gondwe & Masamba, 2014
	Nxaraga				Annual			
	Xakanaxa				Annual			
	Okavango Delta				Annual			Gondwe et al., 2021
					Annual			
					Annual			

a. The average values for the dry (August and February) and wet (May and November) seasons were derived from Table 3 and converted to CO_2-C; the reported error is the standard deviation. b. Ranges were extracted from Figures 6 and 7 using graphreader.com for data, as the data contained only two dry-season measurements, these were treated as wet season averages rather than annual values. Units were converted from kg ha−1 yr−1 to mg m-2 hr-1, with ranges expressed as 95% confidence intervals based on geometric means. c. Data were converted from annual means in units of µmol CO2 m^{-2} sec^{-1}. d. Minimum

(dry season) and maximum (wet) fluxes are reported. e. Data from a field trial, both control (no fertilization) and standard fertilization treatment (according to practice) are reported. f. Data were converted from original units to mg of N or C.

5 Conclusion

This study demonstrated that wetland conversion alters GHG dynamics and soil carbon storage in HVBWs. Conversion shifts emissions from CH_4 to N_2O-dominated fluxes, reflecting major changes in redox potential, microbial processing, and nitrogen cycling. Recovering wetlands partially reestablished SOC stocks but also increased CH_4 emissions, highlighting the strong hydrological control on biogeochemical functioning during wetland recovery.

Although intact HVBWs exhibited comparatively large SOC stocks and low CO_2 fluxes, they also showed elevated CH_4 emissions, emphasizing the important trade-offs among GHG components. These findings illustrate that the net climate effects of wetland conservation and restoration may not be universally beneficial and likely depend on site-specific hydrology, carbon accumulation history, nutrient availability, and recovery trajectories. Given that only one intact HVBW was included in this study, the observed patterns should be interpreted with caution and require validation across broader spatial and temporal scales.

Nevertheless, the results underline the importance of considering full GHG balances together with SOC dynamics when evaluating wetland management strategies. Simplified assumptions that wetland conservation or rewetting inherently results in climate mitigation may overlook substantial variability among systems, particularly in tropical freshwater mineral-soil wetlands, where empirical data remain scarce. These findings therefore provide an important contribution to improving regional and global GHG estimates for tropical wetlands in sub-Saharan Africa.

Declaration of generative AI and AI-assisted technologies

During the preparation of this work, the authors used Paperpal (AI) for grammar checks and word count reduction. We also acknowledge the use of ChatGPT while editing the R-scripts and the use of Perplexity.AI for technical inquiries. After using these tools/services, the authors reviewed and edited the content as needed and take full responsibility for the content of the published article.

Supplement link

Additional information is provided in the Supplementary Material. More data and information are available upon request.

Author contributions

SG, GMG, TH, and SML designed the field experiments and contributed to the conceptualization of the study. TH, GMG, SML, and GW provided overall supervision throughout the study. SG and DGK conducted the field and laboratory investigations and were responsible for data curation and analysis. TH, GMG, and SML contributed to funding acquisition. The first draft of the manuscript was prepared by SG. GMG, TH, SML, and DHZ contributed to methodology, validation, visualization, and final manuscript editing. SG and OO contributed to data analysis, software development, and visualization, with consultation from GMG. All co-authors contributed to the final manuscript through review and editing.

Competing interests

The authors declare that there are no financial, personal, or professional conflicts of interest that could have influenced the research, authorship, or publication of this article

Acknowledgements

The authors gratefully acknowledge Taita Research Station (under University of Helsinki in Kenya) for its support during the fieldwork, as well as Benson Mwakachola for his assistance as a research assistant. The ILRI laboratory staff – especially Paul Mutuo for GHG analysis, Sheila Okoma, Francis, Kelvin, and Collins – are highly appreciated for their assistance, guidance, and support. **SG** gratefully acknowledges her employer, the National Water and Sewerage Corporation Uganda (NWSC), for continued support, with special thanks to Dr. Eng. Sylver Mugisha, Eng. Mahmood Lutaya, and Eng. Andrew Muhwezi. We also thank Emil Holt Bøgh and Anne van Dam for their valuable support and guidance in the statistical analysis. We also appreciate Anne Mette Poulsen for the final edits.

Financial support

This research was supported by the Doctoral Programme of the Austrian Academy of Sciences as part of **SG's** doctoral studies, under grant number 26423. The authors also acknowledge funding from the "Earth observation and environmental sensing for climate-smart sustainable agropastoral ecosystem transformation in East Africa (ESSA)" project funded by the European Union DG International Partnerships under the DeSIRA program (FOOD/2020/418-132 Ref. Ares (2020)7862067-22/122020). **SG** gratefully acknowledge financial support from the Austrian Public Employment Service (AMS). **TH** acknowledges financial support from the Austrian Federal Ministry for Economy, Energy and Tourism and the Christian Doppler Research Association (CD Laboratory MERI). **SML** acknowledges funding from the CGIAR Trust Fund for the Science Programs Sustainable Farming Systems, Multifunctional Landscapes, and Climate Action. **GMG** acknowledges

support from the NNF Starting Grant (NNF22SA0079772) "Sustainable Agriculture in East African Wetlands: Research to Manage Greenhouse Gas Emissions and Soil Carbon Loss (SALSA)".

References

Abrar, M. M., Waqas, M. A., Mehmood, K., Fan, R., Memon, M. S., Khan, M. A., Siddique, N., Xu, M., & Du, J. (2025). Organic carbon sequestration in global croplands: Evidenced through a bibliometric approach. *Frontiers in Environmental Science*, *13*, 1495991. https://doi.org/10.3389/fenvs.2025.1495991

Allen, C. R., Burr, M. D., Camper, A. K., Moss, J. J., & Stein, O. R. (2023). Seasonality, C:N ratio and plant species influence on denitrification and plant nitrogen uptake in treatment wetlands. *Ecological Engineering*, *191*, 106946. https://doi.org/10.1016/j.ecoleng.2023.106946

Anthony, T. L., & Silver, W. L. (2021). Hot moments drive extreme nitrous oxide and methane emissions from agricultural peatlands. *Global Change Biology*, *27*(20), 5141–5153. https://doi.org/10.1111/gcb.15802

Antonijević, D., Hoffmann, M., Zak, D., Prochnow, A., Dubbert, M., Schmidt, M., & Augustin, J. (2025). Impact of plant succession on greenhouse gas fluxes during the transition of a flooded fen peatland. *Communications Earth & Environment*, *6*(1), 611. https://doi.org/10.1038/s43247-025-02607-4

Ascenzi, I., Hilbers, J. P., Van Katwijk, M. M., Huijbregts, M. A. J., & Hanssen, S. V. (2025). Increased but not pristine soil organic carbon stocks in restored ecosystems. *Nature Communications*, *16*(1), 637. https://doi.org/10.1038/s41467-025-55980-1

Ashiq, W., Vasava, H., Ghimire, U., Dunfield, K., Daggupati, P., & Biswas, A. (2022). Seasonal agricultural wetlands act as potential source of N2O and CH4 emissions. *CATENA*, *213*, 106184. https://doi.org/10.1016/j.catena.2022.106184

Bahram, M., Espenberg, M., Pärn, J., Lehtovirta-Morley, L., Anslan, S., Kasak, K., Kõljalg, U., Liira, J., Maddison, M., Moora, M., Niinemets, Ü., Öpik, M., Pärtel, M., Soosaar, K., Zobel, M., Hildebrand, F., Tedersoo, L., & Mander, Ü. (2022). Structure and function of the soil microbiome underlying N2O emissions from global wetlands. *Nature Communications*, *13*(1), 1430. https://doi.org/10.1038/s41467-022-29161-3

Barthel, M., Bauters, M., Baumgartner, S., Drake, T. W., Bey, N. M., Bush, G., Boeckx, P., Botefa, C. I., Dériaz, N., Ekamba, G. L., Gallarotti, N., Mbayu, F. M., Mugula, J. K., Makelele, I. A., Mbongo, C. E., Mohn, J., Mandea, J. Z., Mpambi,

D. M., Ntaboba, L. C., … Six, J. (2022). Low N2O and variable CH4 fluxes from tropical forest soils of the Congo Basin. *Nature Communications*, *13*(1), 330. https://doi.org/10.1038/s41467-022-27978-6

Batson, J., Noe, G. B., Hupp, C. R., Krauss, K. W., Rybicki, N. B., & Schenk, E. R. (2015). Soil greenhouse gas emissions and carbon budgeting in a short-hydroperiod floodplain wetland. *Journal of Geophysical Research: Biogeosciences*, *120*(1), 77–95. https://doi.org/10.1002/2014JG002817

Beillouin, D., Corbeels, M., Demenois, J., Berre, D., Boyer, A., Fallot, A., Feder, F., & Cardinael, R. (2023). A global meta-analysis of soil organic carbon in the Anthropocene. *Nature Communications*, *14*(1), 3700. https://doi.org/10.1038/s41467-023-39338-z

Berendt, J., Jurasinski, G., & Wrage-Mönnig, N. (2023). Influence of rewetting on N2O emissions in three different fen types. *Nutrient Cycling in Agroecosystems*, *125*(2), 277–293. https://doi.org/10.1007/s10705-022-10244-y

Berglund, Ö., Kätterer, T., & Meurer, K. H. E. (2021). Emissions of CO2, N2O and CH4 From Cultivated and Set Aside Drained Peatland in Central Sweden. *Frontiers in Environmental Science*, *9*. https://doi.org/10.3389/fenvs.2021.630721

Beuel, S., Alvarez, M., Amler, E., Behn, K., Kotze, D., Kreye, C., Leemhuis, C., Wagner, K., Willy, D. K., Ziegler, S., & Becker, M. (2016). A rapid assessment of anthropogenic disturbances in East African wetlands. *Ecological Indicators*, *67*, 684–692. https://doi.org/10.1016/j.ecolind.2016.03.034

Bridgham, S. D., Cadillo-Quiroz, H., Keller, J. K., & Zhuang, Q. (2013). Methane emissions from wetlands: Biogeochemical, microbial, and modeling perspectives from local to global scales. *Global Change Biology*, *19*(5), 1325–1346. https://doi.org/10.1111/gcb.12131

Butterbach-Bahl, K., Baggs, E. M., Dannenmann, M., Kiese, R., & Zechmeister-Boltenstern, S. (2013). Nitrous oxide emissions from soils: How well do we understand the processes and their controls? *Philosophical Transactions of the Royal Society B: Biological Sciences*, *368*(1621), 20130122. https://doi.org/10.1098/rstb.2013.0122

Butterbach-Bahl, K., Kiese, R., & Liu, C. (2011). Measurements of Biosphere–Atmosphere Exchange of CH4 in Terrestrial Ecosystems. In *Methods in Enzymology* (Vol. 495, pp. 271–287). Elsevier. https://doi.org/10.1016/B978-0-12-386905-0.00018-8

Butterbach-Bahl, K., Sander, B. O., Pelster, D., & Díaz-Pinés, E. (2016). Quantifying Greenhouse Gas Emissions from Managed and Natural Soils. In T. S. Rosenstock, M. C. Rufino, K. Butterbach-Bahl, L. Wollenberg, & M. Richards (Eds.), *Methods for Measuring Greenhouse Gas Balances and Evaluating Mitigation Options in Smallholder Agriculture* (pp. 71–96). Springer International Publishing. https://doi.org/10.1007/978-3-319-29794-1_4

Climate Watch. (2025). *Greenhouse gas emissions by sector: Agriculture* (Version Processed by Our World in Data) [Dataset]. https://ourworldindata.org/co2/country/kenya

Clough, T. J., Rochette, P., Thomas, S. M., Pihlatie, M., Christiansen, J. R., & Thorman, R. E. (2020). Global Research Alliance N_2O chamber methodology guidelines: Design considerations. *Journal of Environmental Quality*, *49*(5), 1081–1091. https://doi.org/10.1002/jeq2.20117

Convention on Wetlands. (2025). *Global Wetland Outlook 2025: Valuing, conserving, restoring and financing wetlands* (First Edition). Convention on Wetlands. https://doi.org/10.69556/GWO-2025-eng

Delwiche, K. B., Knox, S. H., Malhotra, A., Fluet-Chouinard, E., McNicol, G., Feron, S., Ouyang, Z., Papale, D., Trotta, C., Canfora, E., Cheah, Y.-W., Christianson, D., Alberto, M. C. R., Alekseychik, P., Aurela, M., Baldocchi, D., Bansal, S., Billesbach, D. P., Bohrer, G., … Jackson, R. B. (2021). FLUXNET-CH_4: A global, multi-ecosystem dataset and analysis of methane seasonality from freshwater wetlands. *Earth System Science Data*, *13*(7), 3607–3689. https://doi.org/10.5194/essd-13-3607-2021

Dube, T., Dube, T., & Marambanyika, T. (2023). A review of wetland vulnerability assessment and monitoring in semi-arid environments of sub-Saharan Africa. *Physics and Chemistry of the Earth, Parts A/B/C*, *132*, 103473. https://doi.org/10.1016/j.pce.2023.103473

Elberling, B. B., Kovács, G. M., Hansen, H. F. E., Fensholt, R., Ambus, P., Tong, X., Gominski, D., Mueller, C. W., Poultney, D. M. N., & Oehmcke, S. (2023). High nitrous oxide emissions from temporary flooded depressions within croplands. *Communications Earth & Environment*, *4*(1), 463. https://doi.org/10.1038/s43247-023-01095-8

Ellert, B. H., Janzen, H. H., VandenBygaart, A. J., & Bremer, E. (2007). Measuring change in soil organic carbon storage. In *Soil Sampling and Methods of Analysis* (pp. 25–38). Taylor & Francis Group.

FAO. (2023). *Standard operating procedure for soil bulk density, cylinder method*. FAO. https://doi.org/10.4060/cc7568en

Fluet-Chouinard, E., Stocker, B. D., Zhang, Z., Malhotra, A., Melton, J. R., Poulter, B., Kaplan, J. O., Goldewijk, K. K., Siebert, S., Minayeva, T., Hugelius, G., Joosten, H., Barthelmes, A., Prigent, C., Aires, F., Hoyt, A. M., Davidson, N., Finlayson, C. M., Lehner, B., … McIntyre, P. B. (2023). Extensive global wetland loss over the past three centuries. *Nature*, *614*(7947), 281–286. https://doi.org/10.1038/s41586-022-05572-6

Fowler, A. F., Basso, B., Millar, N., & Brinton, W. F. (2023). A simple soil mass correction for a more accurate determination of soil carbon stock changes. *Scientific Reports*, *13*(1), 2242. https://doi.org/10.1038/s41598-023-29289-2

Garba, S. I., Ebmeier, S. K., Bastin, J.-F., Mollicone, D., & Holden, J. (2025). Wetland fragmentation associated with large populations across Africa. *Nature Communications*, *16*(1), 5065. https://doi.org/10.1038/s41467-025-59373-2

Gardner, R. C., & Finlayson, C. (2018). Global Wetland Outlook: State of the World's Wetlands and Their Services to People. *Ramsar Convention Secretariat, 2018, Stetson University College of Law Researc*, *Paper No. 2020-5*, 89.

Gondwe, M. J., & Masamba, W. R. L. (2014). Spatial and temporal dynamics of diffusive methane emissions in the Okavango Delta, northern Botswana, Africa. *Wetlands Ecology and Management*, *22*(1), 63–78. https://doi.org/10.1007/s11273-013-9323-5

Grebliunas, B. D., & Perry, W. L. (2016). The role of C:N:P stoichiometry in affecting denitrification in sediments from agricultural surface and tile-water wetlands. *SpringerPlus*, *5*(1), 359. https://doi.org/10.1186/s40064-016-1820-6

Gubamwoyo, S., Hein, T., Heiskanen, J., Kisha, D. G., Pellikka, P., Gruber, G., Omondi, V. A., Leitner, S. M., Weigelhofer, G., Mwamodenyi, J. M., Obonyo, A. O., & Gettel, G. M. (2025). Assessing land use changes and agricultural practices in highland valley-bottom wetlands in Taita Hills, Kenya. *Journal of Environmental Management*, *389*, 126122. https://doi.org/10.1016/j.jenvman.2025.126122

Hao, Y., Mao, J., Bachmann, C. M., Hoffman, F. M., Koren, G., Chen, H., Tian, H., Liu, J., Tao, J., Tang, J., Li, L., Liu, L., Apple, M., Shi, M., Jin, M., Zhu, Q., Kannenberg, S., Shi, X., Zhang, X., … Dai, Y. (2025). Soil moisture controls over carbon sequestration and greenhouse gas emissions: A review. *Npj Climate and Atmospheric Science*, *8*(1), 16. https://doi.org/10.1038/s41612-024-00888-8

Hatano, R. (2019). Impact of land use change on greenhouse gases emissions in peatland: A review. *International Agrophysics*, *33*(2), 167–173. https://doi.org/10.31545/intagr/109238

Hochmuth, G., Mylavarapu, R., & Hanlon, E. (2014). Four Rs of Fertilizer Management: SL411/SS624, 10/2014. *EDIS*, *2014*(8). https://doi.org/10.32473/edis-ss624-2014

Hood-Nowotny, R., Umana, N. H.-N., Inselbacher, E., Oswald- Lachouani, P., & Wanek, W. (2010). Alternative Methods for Measuring Inorganic, Organic, and Total Dissolved Nitrogen in Soil. *Soil Science Society of America Journal*, *74*(3), 1018–1027. https://doi.org/10.2136/sssaj2009.0389

Horkel, A., Nauta, W., Niedermayr, G., Okello, R., Pohl, W., & Wachira, J. K. (1979). *GEOLOGY OF THE TAITA HILLS (COAST PROVINCE/KENYA)* (Geological Survey Kenya Report, 102).

Hutchinson, G. L., & Livingston, G. P. (2001). Vents and seals in non-steady-state chambers used for measuring gas exchange between soil and the atmosphere: *Vents and seals for non-steady-state chambers*. *European Journal of Soil Science*, *52*(4), 675–682. https://doi.org/10.1046/j.1365-2389.2001.00415.x

Itoh, M., Okimoto, Y., Hirano, T., & Kusin, K. (2017). Factors affecting oxidative peat decomposition due to land use in tropical peat swamp forests in Indonesia. *Science of The Total Environment*, *609*, 906–915. https://doi.org/10.1016/j.scitotenv.2017.07.132

Jia, M., Blume, O., Amos, R. T., Su, D., Lapen, D. R., & Ulrich Mayer, K. (2022). Assessing GHG cycling in agricultural and riparian soils using a uniform reactive transport modeling approach. *Geoderma*, *425*, 116078. https://doi.org/10.1016/j.geoderma.2022.116078

Jiang, B., Zhang, J., Zhou, G., He, Y., Du, Z., Liu, R., Li, J., Chai, H., Zhou, X., & Chen, H. (2025). Wetland CH4 and CO2 emissions show opposite temperature dependencies along global climate gradients. *CATENA*, *248*, 108557. https://doi.org/10.1016/j.catena.2024.108557

Jones, A., Hiederer, R., & Montanarella, L. (2016). Soil Carbon Map: Africa. In *Encyclopedia of Soil Science* (JRC105552 ed., pp. 2059–2065). Taylor & Francis. https://publications.jrc.ec.europa.eu/repository/handle/JRC105552

Keane, B. J., Ineson, P., Vallack, H. W., Blei, E., Bentley, M., Howarth, S., McNamara, N. P., Rowe, R. L., Williams, M., & Toet, S. (2018). Greenhouse gas emissions from the energy crop oilseed rape (*Brassica napus*); the role of photosynthetically active radiation in diurnal N_2 O flux variation. *GCB Bioenergy*, *10*(5), 306–319. https://doi.org/10.1111/gcbb.12491

Kenya Water Towers Agency. (Not dated). Distribution of Kenya water Towers; Interactive map of Gazetted and Non-Gazetted Water Towers in Kenya. *Kenya Water Towers Agency*. https://watertowers.go.ke/water-towers/

Kluber, L. A., Miller, J. O., Ducey, T. F., Hunt, P. G., Lang, M., & S. Ro, K. (2014). Multistate assessment of wetland restoration on CO2 and N2O emissions and soil bacterial communities. *Applied Soil Ecology*, *76*, 87–94. https://doi.org/10.1016/j.apsoil.2013.12.014

Le Mer, J., & Roger, P. (2001). Production, oxidation, emission and consumption of methane by soils: A review. *European Journal of Soil Biology*, *37*(1), 25–50. https://doi.org/10.1016/S1164-5563(01)01067-6

Li, J., Yuan, J., Dong, Y., Liu, D., Zheng, H., & Ding, W. (2025). Impact of wetland conversion to cropland on ecosystem carbon budget and greenhouse gas emissions in Northeast China. *Agricultural and Forest Meteorology*, *360*, 110311. https://doi.org/10.1016/j.agrformet.2024.110311

Li, L., Awada, T., Shi, Y., Jin, V. L., & Kaiser, M. (2025). Global Greenhouse Gas Emissions From Agriculture: Pathways to Sustainable Reductions. *Global Change Biology*, *31*(1), e70015. https://doi.org/10.1111/gcb.70015

Li, L., Awada, T., Zhang, Y., & Paustian, K. (2024). Global Land Use Change and Its Impact on Greenhouse Gas Emissions. *Global Change Biology*, *30*(12), e17604. https://doi.org/10.1111/gcb.17604

Liu, F., Yang, J., Shen, W., Fu, J., Meng, J., Zhang, Y., Li, J., & Yuan, Z. (2025). Effects of drainage and long-term tillage on greenhouse gas fluxes in a natural wetland: Insights from microbial mechanisms. *Environmental Microbiome*, *20*(1), 26. https://doi.org/10.1186/s40793-025-00682-w

Liu, H., Zak, D., Rezanezhad, F., & Lennartz, B. (2019). Soil degradation determines release of nitrous oxide and dissolved organic carbon from peatlands. *Environmental Research Letters*, *14*(9), 094009. https://doi.org/10.1088/1748-9326/ab3947

Liu, H., Zheng, X., Li, Y., Yu, J., Ding, H., Sveen, T. R., & Zhang, Y. (2022). Soil moisture determines nitrous oxide emission and uptake. *Science of The Total Environment*, *822*, 153566. https://doi.org/10.1016/j.scitotenv.2022.153566

Lynam, J. (2020). The highland perennial farming system: Sustainable intensification and the limits of farm size. In *In Farming Systems and Food Security in Africa* (1st ed., pp. 148–181). Routledge.

Ma, S., Creed, I. F., & Badiou, P. (2024). New perspectives on temperate inland wetlands as natural climate solutions under different CO2-equivalent metrics. *Npj Climate and Atmospheric Science*, *7*(1), 222. https://doi.org/10.1038/s41612-024-00778-z

Malak, A., D., Marin, A. I., Trombetti, M., & Roman San S. (2021). *Carbon pools and sequestration potential of wetlands in the European Union*. European Topic Centre on Urban, Land and Soil Systems. ISBN 978-3-200-07433-0

Mander, Ü., Opik, M., & Espenberg, M. (2025). Global peatland greenhouse gas dynamics: State of the art, processes, and perspectives. *New Phytologist*, n/a-n/a. https://doi.org/10.1111/nph.20436

Marinus, W. (2021). *It's time to harvest! : Towards sustainable farming systems in the East African highlands* [Wageningen University]. https://doi.org/10.18174/554716

Martínez-Espinosa, C., Sauvage, S., Al Bitar, A., Green, P. A., Vörösmarty, C. J., & Sánchez-Pérez, J. M. (2021). Denitrification in wetlands: A review towards a quantification at global scale. *Science of The Total Environment*, *754*, 142398. https://doi.org/10.1016/j.scitotenv.2020.142398

McDaniel, M. D., Saha, D., Dumont, M. G., Hernández, M., & Adams, M. A. (2019). The Effect of Land-Use Change on Soil CH4 and N2O Fluxes: A Global Meta-Analysis. *Ecosystems*, *22*(6), 1424–1443. https://doi.org/10.1007/s10021-019-00347-z

Mganga, K. Z., Sietiö, O.-M., Meyer, N., Poeplau, C., Adamczyk, S., Biasi, C., Kalu, S., Räsänen, M., Ambus, P., Fritze, H., Pellikka, P. K. E., & Karhu, K. (2022). Microbial carbon use efficiency along an altitudinal gradient. *Soil Biology and Biochemistry*, *173*, 108799. https://doi.org/10.1016/j.soilbio.2022.108799

Minamikawa, K., Tokida, T., Sudo, S., Padre, A., & Yagi, K. (2015). *Guidelines for measuring CH_4 and N_2O emissions from rice paddies by a manually operated closed chamber method*. National Institute for Agro-Environmental Sciences.

Mistry, P., Creed, I. F., Trick, C. G., & Lobb, D. A. (2026). Enhanced organic carbon burial in rewetted wetlands precedes long-term stabilization. *Communications Earth & Environment*, *7*(1), 430. https://doi.org/10.1038/s43247-026-03416-z

Mitsch, W. J., Bernal, B., Nahlik, A. M., Mander, Ü., Zhang, L., Anderson, C. J., Jørgensen, S. E., & Brix, H. (2013). Wetlands, carbon, and climate change. *Landscape Ecology*, *28*(4), 583–597. https://doi.org/10.1007/s10980-012-9758-8

Mitsch, W. J., & Gosselink, J. G. (2015). *Wetlands* (Fifth edition). John Wiley and Sons, Inc.

Murguia-Flores, F., Jaramillo, V. J., & Gallego-Sala, A. (2023). Assessing Methane Emissions From Tropical Wetlands: Uncertainties From Natural Variability and Drivers at the Global Scale. *Global Biogeochemical Cycles*, *37*(9), e2022GB007601. https://doi.org/10.1029/2022GB007601

Mwacharo, J. (2024, August). KBAs in Focus – Taita Hills Forests [Nature Kenya]. *KBAs in Focus – Taita Hills Forests*. https://naturekenya.org/2024/08/05/kbas-in-focus-taita-hills-forests/

Nahlik, A. M., & Fennessy, M. S. (2016). Carbon storage in US wetlands. *Nature Communications*, *7*(1), 13835. https://doi.org/10.1038/ncomms13835

Nahlik, A. M., & Mitsch, W. J. (2011). Methane emissions from tropical freshwater wetlands located in different climatic zones of Costa Rica: METHANE EMISSIONS FROM TROPICAL WETLANDS. *Global Change Biology*, *17*(3), 1321–1334. https://doi.org/10.1111/j.1365-2486.2010.02190.x

Nakagawa, S., & Schielzeth, H. (2013). A general and simple method for obtaining R2 from generalized linear mixed-effects models. *Methods in Ecology and Evolution*, *4*(2), 133–142. https://doi.org/10.1111/j.2041-210x.2012.00261.x

Ndah, F. A., Michelsen, A., Rinnan, R., Maljanen, M., Mikkonen, S., & Kivimäenpää, M. (2024). Impact of three decades of warming, increased nutrient availability, and increased cloudiness on the fluxes of greenhouse gases and biogenic volatile organic compounds in a subarctic tundra heath. *Global Change Biology*, *30*(7). https://doi.org/10.1111/gcb.17416

Njana, A. M. (2025). Ecological significance of protected areas in the tropical mountains of Eastern Africa. *Ecological Indicators*, *170*, 113010. https://doi.org/10.1016/j.ecolind.2024.113010

Njeru, C. M., Ekesi, S., Mohamed, S. A., Kinyamario, J. I., Kiboi, S., & Maeda, E. E. (2017). Assessing stock and thresholds detection of soil organic carbon and nitrogen along an altitude gradient in an east Africa mountain ecosystem. *Geoderma Regional*, *10*, 29–38. https://doi.org/10.1016/j.geodrs.2017.04.002

Nyamadzawo, G., Wuta ,Menas, Nyamangara ,Justice, Rees ,Robert M, & and Smith, J. L. (2015). The effects of catena positions on greenhouse gas emissions along a seasonal wetland (dambo) transect in tropical Zimbabwe. *Archives of Agronomy and Soil Science*, *61*(2), 203–221. https://doi.org/10.1080/03650340.2014.926332

Ondiek, R. A., Hayes, D. S., Kinyua, D. N., Kitaka, N., Lautsch, E., Mutuo, P., & Hein, T. (2021). Influence of land-use change and season on soil greenhouse gas emissions from a tropical wetland: A stepwise explorative assessment. *Science of The Total Environment*, *787*, 147701. https://doi.org/10.1016/j.scitotenv.2021.147701

Parkin, T., & Venterea, R.-R. (2010). *USDA-ARS GRACEnet project protocols, chapter 3. Chamber-based trace gas flux measurements. Sampling protocols*. MD.

Pasut, C., Tang, F. H. M., Hamilton, D., Riley, W. J., & Maggi, F. (2021). Spatiotemporal Assessment of GHG Emissions and Nutrient Sequestration Linked to Agronutrient Runoff in Global Wetlands. *Global Biogeochemical Cycles*, *35*(4), e2020GB006816. https://doi.org/10.1029/2020GB006816

Peacock, M., Audet, J., Bastviken, D., Futter, M. N., Gauci, V., Grinham, A., Harrison, J. A., Kent, M. S., Kosten, S., Lovelock, C. E., Veraart, A. J., & Evans, C. D. (2021). Global importance of methane emissions from drainage ditches and canals. *Environmental Research Letters*, *16*(4), 044010. https://doi.org/10.1088/1748-9326/abeb36

Pellikka, P. K. E., Heikinheimo, V., Hietanen, J., Schäfer, E., Siljander, M., & Heiskanen, J. (2018). Impact of land cover change on aboveground carbon stocks in Afromontane landscape in Kenya. *Applied Geography*, *94*(April), 178–189. https://doi.org/10.1016/j.apgeog.2018.03.017

Pellikka, P. K. E., Lötjönen, M., Siljander, M., & Lens, L. (2009). Airborne remote sensing of spatiotemporal change (1955–2004) in indigenous and exotic forest cover in the Taita Hills, Kenya. *International Journal of Applied Earth Observation and Geoinformation*, *11*(4), 221–232. https://doi.org/10.1016/j.jag.2009.02.002

Pinheiro, J., Bates, D., & R Core Team. (2026). *nlme: Linear and Nonlinear Mixed Effects Models* (p. 3.1-170) [Dataset]. https://doi.org/10.32614/CRAN.package.nlme

Platts, P. J., Burgess, N. D., Gereau, R. E., Lovett, J. C., Marshall, A. R., McCLEAN, C. J., Pellikka, P. K. E., Swetnam, R. D., & Marchant, R. (2011). Delimiting tropical mountain ecoregions for conservation. *Environmental Conservation*, *38*(3), 312–324. https://doi.org/10.1017/S0376892911000191

Poulter, B., Bousquet, P., Canadell, J. G., Ciais, P., Peregon, A., Saunois, M., Arora, V. K., Beerling, D. J., Brovkin, V., Jones, C. D., Joos, F., Gedney, N., Ito, A., Kleinen, T., Koven, C. D., McDonald, K., Melton, J. R., Peng, C., Peng, S., …

Zhu, Q. (2017). Global wetland contribution to 2000–2012 atmospheric methane growth rate dynamics. *Environmental Research Letters*, *12*(9), 094013. https://doi.org/10.1088/1748-9326/aa8391

Prananto, J. A., Minasny, B., Comeau, L., Rudiyanto, R., & Grace, P. (2020). Drainage increases CO_2 and N_2O emissions from tropical peat soils. *Global Change Biology*, *26*(8), 4583–4600. https://doi.org/10.1111/gcb.15147

R Core Team. (2024). *A language and environment for statistical computing. R Foundation for Statistical Computing* (Version R 4.4.1) [Computer software]. https://www.R-project.org/

Ramsar Convention on Wetlands. (2018). *Global Wetland Outlook: State of the World's Wetlands and their Services to People*. Ramsar Convention Secretariat.

Rebelo, L.-M., McCartney, M. P., & Finlayson, C. M. (2010). Wetlands of Sub-Saharan Africa: Distribution and contribution of agriculture to livelihoods. *Wetlands Ecology and Management*, *18*(5), 557–572. https://doi.org/10.1007/s11273-009-9142-x

Rheault, K., Christiansen, J. R., & Larsen, K. S. (2024). goFlux: A user-friendly way to calculate GHG fluxesyourself, regardless of user experience. *Journal of Open Source Software*, *9*(96), 6393. https://doi.org/10.21105/joss.06393

Ritchie, H., Rosado, P., & Roser, M. (2020). *Breakdown of carbon dioxide, methane and nitrous oxide emissions by sector*. Our World in Data. https://ourworldindata.org/emissions-by-sector

Rochette, P. (2011). Towards a standard non-steady-state chamber methodology for measuring soil N2O emissions. *Animal Feed Science and Technology*, *166–167*, 141–146. https://doi.org/10.1016/j.anifeedsci.2011.04.063

Rovira, P., Sauras-Yera, T., & Romanyà, J. (2022). Equivalent-mass versus fixed-depth as criteria for quantifying soil carbon sequestration: How relevant is the difference? *CATENA*, *214*, 106283. https://doi.org/10.1016/j.catena.2022.106283

Schuster, L., Taillardat, P., Macreadie, P. I., & Malerba, M. E. (2024). Freshwater wetland restoration and conservation are long-term natural climate solutions. *Science of The Total Environment*, *922*, 171218. https://doi.org/10.1016/j.scitotenv.2024.171218

Schuster, L., Trevathan-Tackett, S., Carnell, P., Morris, K., Mole, B., & Malerba, M. E. (2025). Restoring riparian wetlands for carbon and nitrogen benefits and other critical ecosystem functions. *Journal of Environmental Management*, *391*, 126433. https://doi.org/10.1016/j.jenvman.2025.126433

Shah, A., Huang, J., Han, T., Khan, M. N., Tadesse, K. A., Daba, N. A., Khan, S., Ullah, S., Sardar, M. F., Fahad, S., & Zhang, H. (2024). Impact of soil moisture regimes on greenhouse gas emissions, soil microbial biomass, and enzymatic activity in long-term fertilized paddy soil. *Environmental Sciences Europe*, *36*(1), 120. https://doi.org/10.1186/s12302-024-00943-4

Shi, J., Deng, L., Wu, J., Bai, E., Chen, J., Shangguan, Z., & Kuzyakov, Y. (2024). Soil Organic Carbon Increases With Decreasing Microbial Carbon Use Efficiency During Vegetation Restoration. *Global Change Biology*, *30*(12), e17616. https://doi.org/10.1111/gcb.17616

Simango, K. (2024). *Africa's Mountains: Pillars of Life, Livelihoods, and Sustainability - AfriCGE*. https://africancentre.org/africas-mountains-pillars-of-life-livelihoods-and-sustainability/

Taita Taveta County Government. (2023). *County Integrated Development Plan III 2023-2027*. https://maarifa.cog.go.ke/sites/default/files/2024-06/TAITA%20TAVETA%20CIDP%202023-2027.pdf

Tan, L., Ge, Z., Ji, Y., Lai, D. Y. F., Temmerman, S., Li, S., Li, X., & Tang, J. (2022). Land use and land cover changes in coastal and inland wetlands cause soil carbon and nitrogen loss. *Global Ecology and Biogeography*, *31*(12), 2541–2563. https://doi.org/10.1111/geb.13597

Tan, L., Ge, Z., Zhou, X., Li, S., Li, X., & Tang, J. (2020). Conversion of coastal wetlands, riparian wetlands, and peatlands increases greenhouse gas emissions: A global meta-analysis. *Global Change Biology*, *26*(3), 1638–1653. https://doi.org/10.1111/gcb.14933

Tangen, B. A., & Bansal, S. (2020). Soil organic carbon stocks and sequestration rates of inland, freshwater wetlands: Sources of variability and uncertainty. *Science of The Total Environment*, *749*, 141444. https://doi.org/10.1016/j.scitotenv.2020.141444

Tian, H., Xu, X., Lu, C., Liu, M., Ren, W., Chen, G., Melillo, J., & Liu, J. (2011). Net exchanges of CO2, CH4, and N2O between China's terrestrial ecosystems and the atmosphere and their contributions to global climate warming. *Journal of Geophysical Research: Biogeosciences*, *116*(G2). https://doi.org/10.1029/2010JG001393

Turetsky, M. R., Kotowska, A., Bubier, J., Dise, N. B., Crill, P., Hornibrook, E. R. C., Minkkinen, K., Moore, T. R., Myers-Smith, I. H., Nykänen, H., Olefeldt, D., Rinne, J., Saarnio, S., Shurpali, N., Tuittila, E.-S., Waddington, J. M., White,

J. R., Wickland, K. P., & Wilmking, M. (2014). A synthesis of methane emissions from 71 northern, temperate, and subtropical wetlands. *Global Change Biology*, *20*(7), 2183–2197. https://doi.org/10.1111/gcb.12580

Ueyama, M., Fujimoto, A., Ito, A., Takahashi, Y., & Ide, R. (2021). Constraining models for methane oxidation based on long-term continuous chamber measurements in a temperate forest soil. *Agricultural and Forest Meteorology*, *310*, 108654. https://doi.org/10.1016/j.agrformet.2021.108654

van Dam, A. A., Kipkemboi, J., Rahman, M. M., & Gettel, G. M. (2013). Linking Hydrology, Ecosystem Function, and Livelihood Outcomes in African Papyrus Wetlands Using a Bayesian Network Model. *Wetlands*, *33*(3), 381–397. https://doi.org/10.1007/s13157-013-0395-z

Venterea, R. T., Spokas, K. A., & Baker, J. M. (2009). Accuracy and Precision Analysis of Chamber-Based Nitrous Oxide Gas Flux Estimates. *Soil Science Society of America Journal*, *73*(4), 1087–1093. https://doi.org/10.2136/sssaj2008.0307

von Haden, A. C., Yang, W. H., & DeLucia, E. H. (2020). Soils' dirty little secret: Depth-based comparisons can be inadequate for quantifying changes in soil organic carbon and other mineral soil properties. *Global Change Biology*, *26*(7), 3759–3770. https://doi.org/10.1111/gcb.15124

Vymazal, J. (2025). Nitrogen removal in constructed wetlands. *Current Opinion in Environmental Science & Health*, *48*, 100668. https://doi.org/10.1016/j.coesh.2025.100668

Wagner, D. (2017). Effect of varying soil water potentials on methanogenesis in aerated marshland soils. *Scientific Reports*, *7*(1), 14706. https://doi.org/10.1038/s41598-017-14980-y

Wangari, E. G., Mwanake, R. M., Kraus, D., Werner, C., Gettel, G. M., Kiese, R., Breuer, L., Butterbach-Bahl, K., & Houska, T. (2022). Number of Chamber Measurement Locations for Accurate Quantification of Landscape-Scale Greenhouse Gas Fluxes: Importance of Land Use, Seasonality, and Greenhouse Gas Type. *Journal of Geophysical Research: Biogeosciences*, *127*(9). https://doi.org/10.1029/2022JG006901

Were, D., Kansiime, F., Fetahi, T., & Hein, T. (2021). Carbon Dioxide and Methane Fluxes from Various Vegetation Communities of a Natural Tropical Freshwater Wetland in Different Seasons. *Environmental Processes*, *8*(2), 553–571. https://doi.org/10.1007/s40710-021-00497-0

Wu, D., Zhao, C., Bai, H., Feng, F., Sui, X., & Sun, G. (2021). Characteristics and metabolic patterns of soil methanogenic archaea communities in the high-latitude natural forested wetlands of China. *Ecology and Evolution*, *11*(15), 10396–10408. https://doi.org/10.1002/ece3.7842

Xu, S., Liu, X., Li, X., & Tian, C. (2019). Soil organic carbon changes following wetland cultivation: A global meta-analysis. *Geoderma*, *347*, 49–58. https://doi.org/10.1016/j.geoderma.2019.03.036

Yang, T., Jiang, J., He, Q., Shi, F., Jiang, H., Wu, H., & He, C. (2025). Impact of drainage on peatland soil environments and greenhouse gas emissions in Northeast China. *Scientific Reports*, *15*(1), 8320. https://doi.org/10.1038/s41598-025-92655-9

Zheng, X., Xie, B., Liu, C., Zhou, Z., Yao, Z., Wang, Y., Wang, Y., Yang, L., Zhu, J., Huang, Y., & Butterbach-Bahl, K. (2008). Quantifying net ecosystem carbon dioxide exchange of a short-plant cropland with intermittent chamber measurements: NEE QUANTIFICATION OF A CROPLAND. *Global Biogeochemical Cycles*, *22*(3), n/a-n/a. https://doi.org/10.1029/2007GB003104

Zuur, A. F., & Ieno, E. N. (2016). A protocol for conducting and presenting results of regression-type analyses. *Methods in Ecology and Evolution*, *7*(6), 636–645. https://doi.org/10.1111/2041-210X.12577

Zuur, A. F., Ieno, E. N., & Smith, G. M. (2007). *Analysing Ecological Data*. Springer New York. https://doi.org/10.1007/978-0-387-45972-1